2011

Investigation of Solid-State Shear Pulverization Processing Parameters for Polyethylene-Clay Nanocomposites

Ben Aldrich
Bucknell University

Investigation of Solid-State Shear Pulverization Processing Parameters for Polyethylene-Clay Nanocomposites

by

Benjamin D. Aldrich

A Thesis Submitted to the Honors Council

For Honors in the Department of Chemical Engineering

May 12, 2011

Approved by:

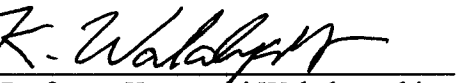

Adviser: Professor Katsuyuki Wakabayashi

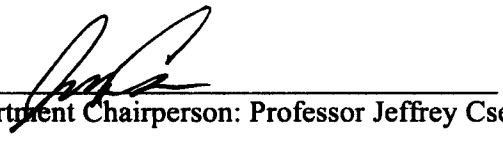

Department Chairperson: Professor Jeffrey Csernica

Acknowledgements

First and foremost, I want to thank my advisor and friend, Professor Kat Wakabayashi, for his support, guidance, and interest in my well-being and success. I am forever grateful for everything that he has helped me with this year and throughout my Bucknell career. I consider him one of my closest friends and hold him in the utmost esteem. That he accepted me to be his Honor's Thesis student meant a great deal to me.

In a year that began with me returning from my semester abroad and will end with me returning to England for my graduate studies, Kat has been *the* pillar of support on which I have relied. His candid and intimate advice always forced me to ask the right questions and directed me in the right direction. Though I never had Kat as a lecturing professor, I feel that I have learned more from him than any other person in my time at Bucknell. He is singlehandedly responsible for teaching me 'the art of professionalism', and has always emphasized ethics, virtue, perseverance, diligence and responsibility.

Kat is a special person. Never have I met a person who puts more effort into teaching than he does. Never have I had, or heard about, a professor who cares more about the well-being of his students than he does. He does not give generic advice. He does not answer questions without learning about the student and the situation. Bucknell is incredibly lucky to have him as a faculty member and I am incredibly luckily to have had in my in life.

Kat's golf game could definitely improve—though he would argue that as he's won all three ChemE Cups, it probably can't—and he could definitely learn a thing or

two from Professor Snyder about playing Settlers of Catan. He has few other weaknesses. That I am able to make these claims with extreme confidence shows how available Kat has made himself to the student body at Bucknell. He's not just a professor; he is a friend and mentor. He is *my* friend and mentor. The countless hours that Kat and I have spent together have, admittedly, been stressful at times, but the fun we have had and what I have learned from him far outweigh the difficulties. I am a better man for having known him.

I would be remiss if I did not thank Alex Fielding (2011) for being Kat's graduate student. That I had someone to, for lack of a better phrase, complain about Kat to, helped keep me sane over the course of the year. I have considered Alex a close friend of mine since I started with the Polymer Hybrid Technology Lab, and I could not have imagined a better companion for this voyage. He has always been more than willing to help me with research, but more importantly has always been there with life advice when I needed it. I am also indebted to my other research colleagues, both past and present, who have supported me, educated me, and aided me with this thesis. Of special note are Marc Henry (2010), without whom the SSSP would still be a mysterious black box, and Mike Boches (2012) and Alyssa Whittington (2014), both of whom have ably assisted me and shared test results over the past year. I wish Alex, Marc, Mike and Alyssa the best of luck in their future endeavors.

This thesis would not have been possible without the help of Diane Hall or Brad Jordan, the former always providing me with any material or equipment I needed and the

latter assisting me with X-ray diffraction testing in the week before this thesis was to be submitted.

Lastly, I want to thank those individuals who always provided me with an excuse not to do research. You know who you are. Your many distractions, in the form of golf, Mario Tennis, Settlers of Catan, Chinese food, drinking, and casino trips, made doing lab work and writing this thesis all the more difficult. They also made my senior year unforgettable. Thank you for preserving my sanity.

Table of Contents

List of Figures

List of Tables

Abstract

Polymer nanocomposites (PNCs) are advanced materials that contain small amounts of nanoscale fillers dispersed in a polymer matrix. These fillers can greatly enhance the physical properties of the resulting composites, such as mechanical stiffness and toughness, thermal stability, electrical conductivity, chemical resistance, and reduced gas permeability. Such potential property improvements in polymer nanocomposites lead to a wide range of high-performance applications, from packaging to automotive parts and sporting goods.

There are several widely-used techniques to produce polymer nanocomposites, each of which has distinct advantages and disadvantages. One process, extrusion, has the potential to be applied to mass production of nanocomposites, but the high-temperature processes can lead to practical issues like polymer degradation and filler re-agglomeration. An alternative to melt-state fabrication is solid-state processing, which has been gaining popularity in the research community. This relatively novel method applies high amounts of shear and compressive forces carried out at temperatures below the melt and/or glass transition temperature of the polymer. Solid-state shear pulverization (SSSP) is a continuous solid-state milling technique in which polymer/nanofiller blends are pulverized within a modified twin-screw extruder operating at sub-ambient temperatures The SSSP method can be tailored to specific applications by controlling the numerous processing parameters. Additionally, solid-state shear

pulverization can be followed by melt processing so that it can be molded into the designed shape.

This Honor's thesis investigates multiple processing parameters, including polymer type, filler type, processing technique, severity of SSSP processing, and post-processing, of SSSP. HDPE and LLDPE polymers with pristine clay and organo-clay samples are explored. Effects on crystallization, high-temperature behavior, mechanical properties, and gas barrier properties are examined. Thermal, mechanical, and morphological characterization is conducted to determine polymer/filler compatibility and superior processing methods for the polymer-clay nanocomposites.

This study shows that inclusion of a filler is more beneficial to less crystalline LLDPE than to highly crystalline HDPE. With regards to the filler type, organo-clay is no better suited for processing of PNCs than pristine clay is. Greater property enhancements are seen in pristine clay samples compared to the respective organo-clay samples; specifically, pristine clay appears to be more a compatible filler with LLDPE. Furthermore, there is a noticeable difference in the material properties of PNCs fabricated under harsh and mild SSSP conditions; while harsh processing yields enhanced permeability properties, mild processing yields improved mechanical characteristics. Lastly, extrusion following SSSP is shown to deteriorate material properties that had previously been improved via SSSP processing.

1. Introduction

Since the early 1900's, polymeric materials, predominantly in the form of plastics and rubbers, have emerged as a synthetic alternative to metals, ceramics, and other naturally-derived materials [1]. Polymers are high molecular weight organic molecules with repeat units made of carbon, oxygen, nitrogen, hydrogen, and other elements. They can be tailored to nearly every application depending on the size and nature of the molecule. They are commonly mass-produced from petroleum-derived chemicals and are traditionally inexpensive to fabricate. One primary advantage of polymers is that they are moldable to almost any shape due to their relatively low melting and softening (called glass transition) temperatures. In addition, polymers are often soft and ductile but at the same time stiff and sturdy at room temperature, which is the reason that polymers are prevalent in many applications. However, polymers typically lack the strength and high-temperature behavior of typical metals and ceramics, making them imperfect substitutes for strenuous applications.

Polymeric materials are often mixed with high-performance additives so that the original properties are enhanced; these additives are termed fillers and range from minerals to ceramics to metals. When one incorporates fillers in polymers, one can generate a virtually infinite variety of materials with superior physical properties and competitive production costs. Thermal stability, mechanical strength, and gas barrier properties are some example characteristics that can be drastically improved through the addition of fillers. Nanofillers—fillers in which at least one of the dimensions measures

less than 100 nanometers—have significant advantages over traditional macro-scale fillers due to a much greater surface area to volume ratio. This means that less filler can be added to the polymer matrix, or polymer base, while still allowing the bulk properties of the polymer to be retained.

While additives typically enhance the material properties of the polymer, the extent to which the addition of the filler is effective is dependent on polymer processing techniques achieving high levels of dispersion (spread) and exfoliation (separation). There are several traditional fabrication techniques typically employed in industry, but each has serious drawbacks. Solid-state shear pulverization (SSSP) is a relatively new technique that grinds polymers and fillers together well below the melt temperature of the polymer; SSSP avoids the use of expensive and/or dangerous solvents, does not thermally degrade the polymer or filler, and is a continuous process well suited for industry. Solid-state shear pulverization has been shown to be an effective polymer nanocomposite processing method, capable of achieving high levels of dispersion and exfoliation within the sample.

In this Honors thesis, fabrication and characterization of polymer nanocomposites (PNCs) will be considered using high-density polyethylene (HDPE) and linear low-density polyethylene (LLDPE) as the polymers and pristine and organically modified (organo-) clays as nanofillers. Polyethylene is among the most common plastics in society, with applications ranging from milk jugs to plastic bags [2, 3]. Clays, specifically pristine clay and organo-clay, are currently considered the most typical

nanofiller in the research community. HDPE and LLDPE, and pristine and organo-clay are considered the most fundamental choice of polymer and filler, respectively, and therefore are fundamental to ensuing research. This report aims to compare the mechanical and morphological properties of PNCs processed via heated extrusion, SSSP, and solid-state shear pulverization followed by heated extrusion. Direct comparison of the processing methods will serve as a good model study for all future polymer nanocomposites.

This thesis first describes the current fabrication processes used in literature and industry. Nanocomposite materials will be discussed along with previously published methods for polymer nanocomposite preparation. The materials and methods section will identify materials to be used in experiments as well as sample preparation and testing methods. The results section will report major findings concerning the PNCs, and will compare physical, mechanical, thermal, and permeation properties of the polymer nanocomposites produced via different processing techniques. The results will be analyzed using binary comparisons in the discussion section, and conclusions will be drawn from these results to demonstrate the viability of SSSP in producing polymer nanocomposites, the contrasting effects of pristine vs. organo-clay, and the effect of post-SSSP extrusion on polyethylene-clay system. Lastly, major conclusions and recommendations for future studies will be provided.

2. Background

2.1 Polyethylene

Polyethylene (PE) is one of the most widely used polymers, with applications ranging from milk jugs and detergent bottles, made from high-density polyethylene (HDPE), to film and bubble wraps, made from linear low-density polyethylene (LLDPE) [3, 4]. The basic repeat unit of PE is shown in Figure 1. Polyethylene is an extremely versatile polymer. It generally has high toughness and ductility, excellent chemical resistance, low water vapor permeability, and very low water absorption [3]. These properties combined with the ease of processing make PE one of the highest-volume polymers in the world; nearly 80 million metric tons of PE are produced each year [5, 6]. Properties of PE can be varied widely by controlling the molecular weight, the molecular weight distribution, and the length and degree of branching [4]. PE can be classified into multiple categories based on density and branching. Three distinctive and influential PE subsets are shown in Figure 2: high-density polyethylene (HDPE), low-density polyethylene (LDPE), and linear low-density polyethylene (LLDPE). HDPE is comprised of densely packed polymer strands as there is almost no branching in the polymer ($\rho \geq 0.941$ g/cm^3). LDPE has a higher degree of branching and far longer branches than HDPE and therefore packs the less densely ($\rho = 0.910$-0.940 g/cm^3). Linear low-density polyethylene has more branching than HDPE but differs structurally from conventional low-density polyethylene because of the absence of long chain branching ($\rho = 0.915$-0.925 g/cm^3) [3].

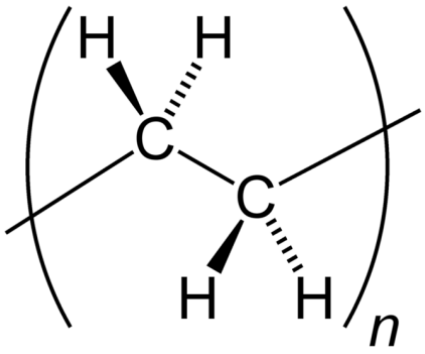

Figure 1. Polyethylene (PE) repeat unit.

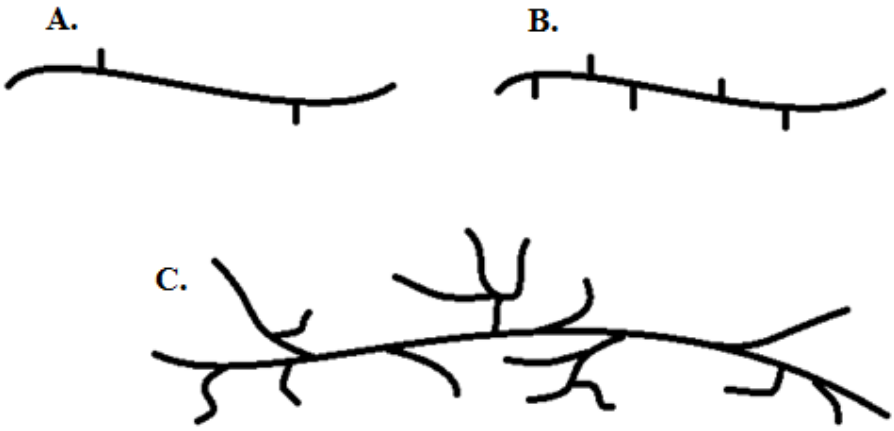

Figure 2. Comparing branching of A. High-Density Polyethylene (HDPE), B. Linear Low-Density Polyethylene (LLDPE), and C. Low-Density Polyethylene [3].

Mechanical properties of PE depend significantly on variables such as the extent of branching, as well as the crystalline structure and molecular weight of the polymer. All polyethylenes are relatively soft, and hardness increases as density increases; generally, as the density of the polymer increases, dimensional stability and physical properties improve, especially at high temperatures [3].

Due to varying branch content and density, HDPE has stronger intermolecular forces and therefore tensile strength, while LDPE has high impact strength, toughness,

and ductility [4]. As such, LDPE is commonly used as protective sheeting [3, 4]. Conventional LLDPE differs from LDPE by having a narrower molecular weight distribution and by not containing long-chain branching, as shown in Table 1. LLDPE is a substantially linear polymer with significant numbers of short branches and has enhanced tensile strength for the same density as LDPE because of stronger intermolecular forces [3, 4].

Table 1. Typical Weight Average Molecular Weights of Three Types of Polyethylene [3-6].

Type of Polyethylene	***Molecular Weight (g/mol)***
High Density Polyethylene (HDPE)	20,000-1,000,000+
Low Density Polyethylene (LDPE)	70,000-120,000
Linear-Low Density Polyethylene (LLDPE)	82,000-107,000

As can be seen above, PEs are versatile in structure and properties, and are used in many applications. However, as polymeric materials continue to replace metals and ceramics in the society, there is a need to enhance the base performance of commodity polymers like PE.

2.2 Polymer Nanocomposites

Polymeric materials are often mixed with other high-performance additives to enhance their base material properties; when combined with additives, one can generate a virtually infinite variety of materials with unique physical properties and competitive production costs [2, 7, 8]. These additives can range from minerals to ceramics, and are termed fillers. These materials are called polymer composite systems. Automobile tires

are an everyday example of composites; the base rubber is called the polymer matrix, while the carbon black additive is the dispersed particle phase and acts as a reinforcing agent. The filler functions to conduct heat away from the tread and belt area of the tire, reducing thermal damage and increasing tire life. Fillers range in size, shape, and chemistry, which dictate the resulting composite performance. When the fillers are small—one of the dimensions of the filler measuring less than 100 nm—the filler is called a nanofiller, and the system is termed polymer nanocomposite (PNC).

Polymer nanocomposites have been the focus of many studies over the past two decades because of their potential to dramatically enhance or impart unique material properties [9-18]. PNCs represent the current trend in novel nanostructured materials [8]. PNCs have many advantages over traditional polymeric materials. The addition of nanoscale fillers to polymers at even small volume fraction can yield various physical property enhancements such as mechanical strength, thermal stability, electrical conductivity, gas barrier properties, and flame retardancy. The bulk properties can be controlled and tuned based on the type of loading percentage (amount added) of the filler. For example, PNCs can be used in packaging applications because of the nanofiller's ability to enhance gas barrier properties. Impermeable nanofiller platelets exfoliated and dispersed throughout the polymer matrix create a tortuous pathway for gas and vapor permeants diffusing through the nanocomposite, as shown in Figure 3 [19, 20].

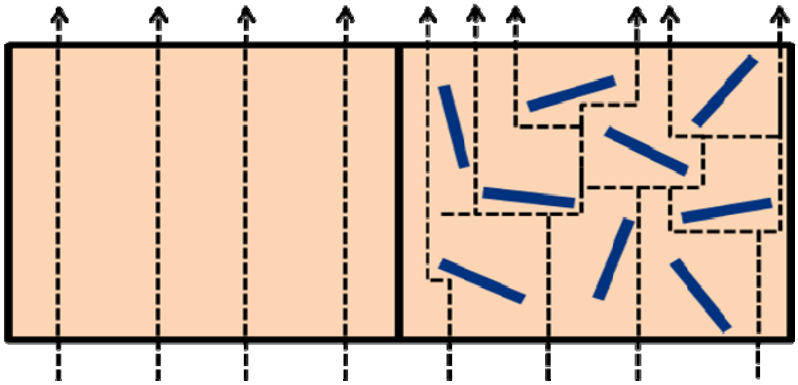

Figure 3. Schematic of tortuous path mechanism introduced by clay sheets in polymer-clay nanocomposites. The left frame indicates the non-obstructed paths of permeants (dotted lines). The right frame indicates the longer path lengths traveled by diffusing molecules after being obstructed by clay nanosheets (blue rectangles) [21].

The physical properties of PNC systems are a related to the surface area of the filler within the polymer matrix; significant impact arises from the large surface to volume ratio provided by the nanoparticles resulting in significant polymer-nanofiller interfacial interactions altering the properties of the polymer matrix [12, 14, 17, 18]. Therefore, less filler must be added to achieve the same filler surface area, as shown in Figure 4. Furthermore, PNCs can be prepared at rather low costs because of the reduction in the required amount of filler.

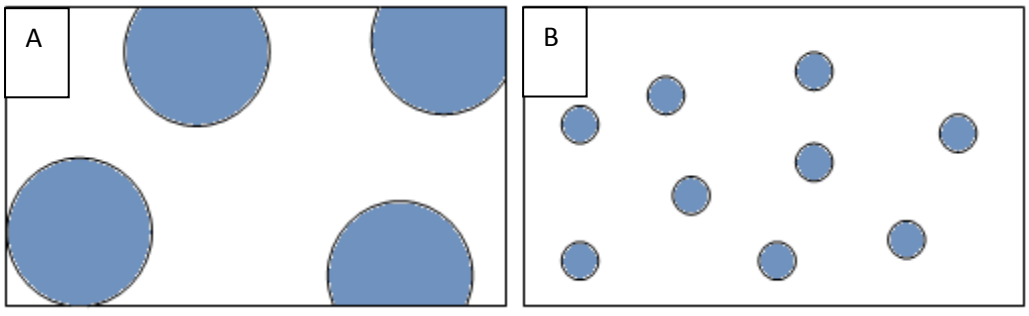

Figure 4. Comparing surface area to volume ratio for macro-scale fillers (A) and nano-scale fillers (B). A and B have the same surface area but B has much less filler volume.

2.3 Processing

Fabrication of PNCs involves some kind of mixing process which combines the filler and the matrix polymer and the shaping of the sample into a final specimen or product. This is referred to as processing. There are two key processing criteria must be met when fabricating polymer nanocomposites: dispersion and exfoliation. Dispersion refers to the spread of the filler throughout the polymer matrix, while exfoliation refers to the separation of individual nanofiller sheets. The two terms are represented pictorially below in Figure 5. Nanofillers are more thermodynamically stable if they remain aggregated of clumped together, which means that during processing, it is very difficult to separate the filler particles. Only effective processing results in high levels of dispersion and exfoliation, two morphological states that are essential in achieving outstanding improvements in material properties [12].

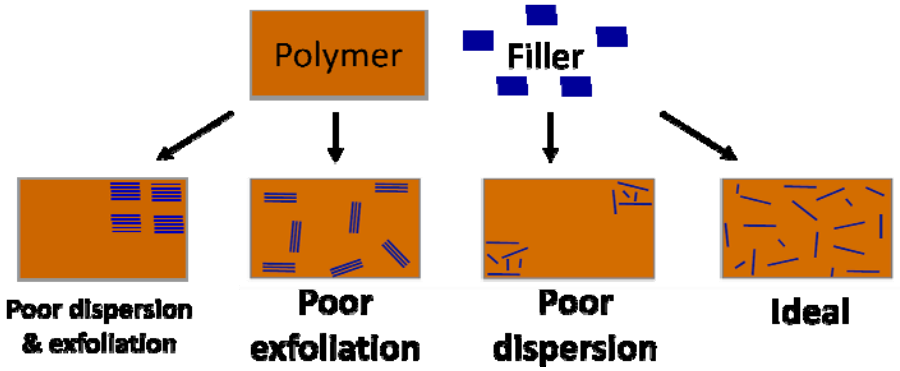

Figure 5. Dispersion (spread) and exfoliation (separation).

There are several processing techniques currently used in industry to produce polymer nanocomposites. Solution-mixing combines the nanofillers and the polymer in the presence of a solvent and in situ polymerization polymerizes the monomer in the

presence of dispersed nanofillers. Melt mixing is a process where the polymer is simply melted and the nanofillers are mixed in.

The morphology requirements for successful PNCs are not easy to achieve; however, each of the processing techniques listed above is capable of achieving various levels of morphological and material property enhancements. It has been shown that the conductivity of carbon nanotube PNCs was enhanced using solution intercalation method [22]. Improved levels of dispersion of carbon nanotubes have been achieved by in situ polymerization under sonication [23]. Both solution intercalation [24-26] and in situ polymerization [27-32] of PNCs are common laboratory scale techniques incapable of addressing the requirements of producing PNCS at an industrial scale due to limited reactor size, cost, and use of potentially dangerous solvents. In order to meet the high throughput demands of industrial manufacturing, melt mixing [32-36] has received considerable attention [14], making it the most common technique used in industry.

Each of these methods has inherent flaws. Solution-mixing is limited to small-scale operations because of the large requirement of solvents. In situ polymerization is limited by the selection of filler-monomer pairs and the use of monomers is not environmentally benign. Melt mixing can lead to thermal degradation of the polymer due to the high temperatures [2, 12, 37]. Additionally, as filler dispersion and separation is not stable, it is thermodynamically favorable for the fillers to agglomerate. Melt mixing produces a high energy environment that encourages this re-agglomeration [2, 12, 37].

The Polymer Hybrid Nanotechnology Laboratory at Bucknell University explores a fourth, rather novel method: solid-state shear pulverization (SSSP). Recently, this process was shown to yield fine nanoscale dispersion and substantial exfoliation levels, two structural conditions indicative of a successful fabrication technique [11, 12, 14, 37].

2.4 Solid-State Shear Pulverization

Solid-state processing combines the polymer and nanofiller in the solid phase. This is achieved by processing at low temperature and applying shear and compressive forces to crush the polymer and the nanofillers into a fine powder. This effectively disperses the nanofillers and ensures uniform behavior in the sample. By operating at a low temperature, below the melt and/or glass transition temperature of the polymer, the SSSP maintains a low energy environment for the nanofiller to avoid re-agglomerating. The advantage of this processing technique is that it is an industrially applicable process free of harmful or dangerous solvents, unlike solution-mixing or in situ polymerization. Furthermore, it ensures good dispersion of the filler, unlike melt mixing.

Torkelson's research group at Northwestern University has developed the SSSP technique and has shown that SSSP is an improved fabrication technique over melt mixing, in situ polymerization, or solution intercalation. Northwestern has been able to achieve multiple material property enhancements such as improved tensile strengths, higher degradation temperature and reduced permeation properties [8, 11, 12, 14]. As an example, Torkelson et al. have shown improvements in mechanical properties and

degradation temperatures for polypropylene/carbon nanotube systems when comparing SSSP-ed samples to as obtained polypropylene and melt-mixed samples.

A recent paper from Masuda and Torkelson reported on the fabrication of polypropylene-carbon nanotube PNCs via SSSP and showed that the PNC crystallization rate increased by three-fold in comparison to the samples made via melt mixing [14]. In a separate study, Wakabayashi and Torkelson varied the amount of graphite in polypropylene and demonstrated increased degradation temperatures and mechanical properties in the PNCs fabricated by SSSP [11]. While these improvements were expected, Wakabayashi's study demonstrates the ability of SSSP to improve material characteristics. However, there is still limited understanding and much less control over the state of filler dispersion in the host polymer [14].

Solid-state fabrication of PNCs has also been explored by Wakabayashi et al. in Bucknell University's Polymer Hybrid Nanotechnology Lab [12, 13] using a state of the art solid-state shear pulverizer [38].

2.5 Post-SSSP Processing Studies

SSSP has demonstrated that material property enhancements can be achieved for a wide range of PNCs. There remain questions, however, as to how the characteristics of the SSSP product, a fine powder, will change when heat is applied to mold the powder into usable shapes and products. Does applying heat undo the high levels of dispersion

and exfoliation achieved with SSSP techniques? Does applying heat on top of harsh SSSP conditions thermally degrade the product?

Masuda and Torkelson of Northwestern University have examined the effects of post-SSSP melt mixing for polypropylene-carbon nanotube PNCs. Post-SSSP melt mixing is a two step process; samples are first processed by SSSP into a powder and then the powder is melt-mixed into a strand. Their results show that the material properties are altered in a positive way as they were able to achieve higher levels of dispersion than by SSSP only [11]. The PP-carbon nanotube systems studied showed increases in the Young's modulus and yield strength when comparing MM only and SSSP only to SSSP-MM [11]. The study found that two step SSSP-MM processing yields dispersion that is a function of CNT dimensions and entanglements in the as-received state. One major finding of the study was that to achieve excellent dispersion, the two-step process must be tailored to CNT characteristics. Additionally, isothermal crystallization studies showed that the PNC made by two-step processing exhibited a symmetric, sharp crystallization curve, which reflects its homogeneous dispersion, and that the isothermal crystallization curves for MM, SSSP and SSSP-MM are consistent with the superior dispersion achieved by two-step processing [11]. Thermal stability was also shown to increase as dispersion improves, with the degradation temperature of the polymer samples improved by 27 °C for SSSP-MM [11].

It would be useful to verify if this post-melt mixing process is applicable in other types if PCNs which provides the impetus for my research with PE polymers.

3. Materials and Methodology

The following chapter describes the materials and methods, both fabrication and analysis, used to conduct this research.

3.1 Materials

This study involved the processing of two types of polymeric materials and two types of clay fillers. One type of high-density polyethylene (HDPE) was used in this study: Lyondell LR7320 (indentified in this thesis as HDPE7320, melt index 0.3 g/10 min, ρ=0.953 g/cm^3) [39]. In addition, one type of linear low-density polyethylene (LLDPE) was used in this study: DOW Dowlex 2027G (LLDPE2027, melt index 4.0 g/10 min, ρ=0.941 g/cm^3) [40]. Both polymers are polyethylene, whose repeat unit structure is shown in Figure 1, but they differ in the synthesis methods; LLDPE production leads to significant short chain branching, as seen in Figure 2. HDPE is stiffer and harder due to the prominence of crystals in the matrix and the densely packed nature of the polymer strands.

Two types of montmorillonite clay fillers were used in this experiment: as-received montmorillonite, termed pristine, clay (Nanocor Nanomer PGW) and organically modified, termed organo-, clay (Southern Clay Products Cloisite 15A). Montmorillonite-based clays are composed of various silicates, which are minerals containing a silicon anion. Structurally, montmorillonite is comprised of an octahedral silicate crystal sheet sandwiched between two tetrahedral silicate crystal sheets [9, 41-44] as shown in Figure 6. The structure of clay is layered repeated sheets of inorganic

materials. In its pristine state, it is organophobic and therefore is not compatible with polymer. Cloisite 15A is a natural montmorillonite modified with an ammonium salt [45] rendering the clay organophilic. Depending on the functionality, packing density and length of the organic modifiers, the organo-clay can be engineered to optimize their compatibility with a given polymer [46]. The fillers were purchased from commercial vendors and received in micron size particles. When processed with polymers, the fillers are broken down to the nanoscale.

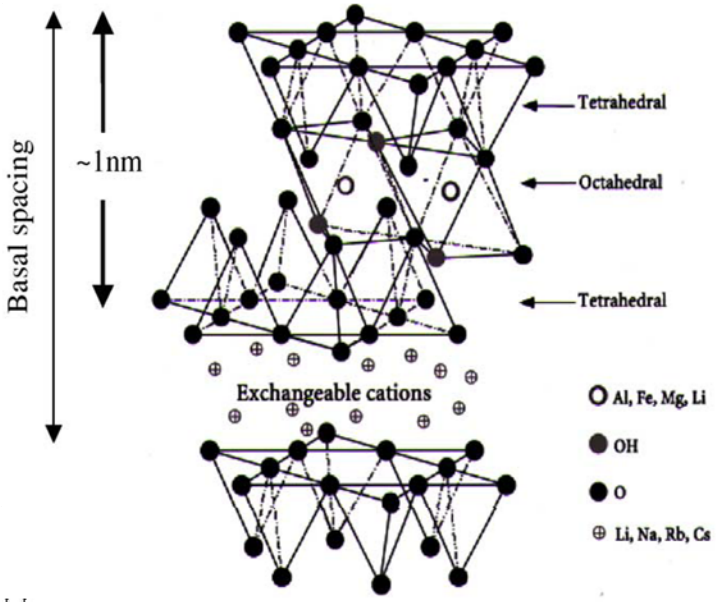

Figure 6. Structure of montmorillonite clay showing the silicate sheets [47].

3.2 Processing

Several means of processing polymer nanocomposites were employed in this experiment. The three techniques are described in detail below.

3.2.1 Twin-Screw Extrusion (TSE)

Twin-Screw Extrusion (TSE) is a continuous and industrially-applicable processing method. As seen in Figure 7, the barrel of a twin-screw extruder is heated with electric heaters to well above the melting temperature of the polymer matrix. The nanofillers are added to the TSE instrument with the polymer matrix and are mixed into the matrix phase. The specially designed screws, which can be custom-configured to tailor to desired outcomes, push the material down a barrel and impart high shear forces which mix the polymeric matrix and filler. The product of twin-screw extrusion is a polymer strand that can later be pressed into sheets. The PNC strand is often cut using scissors or a pelletizer (automatic cutter) into small segments for easier pressing.

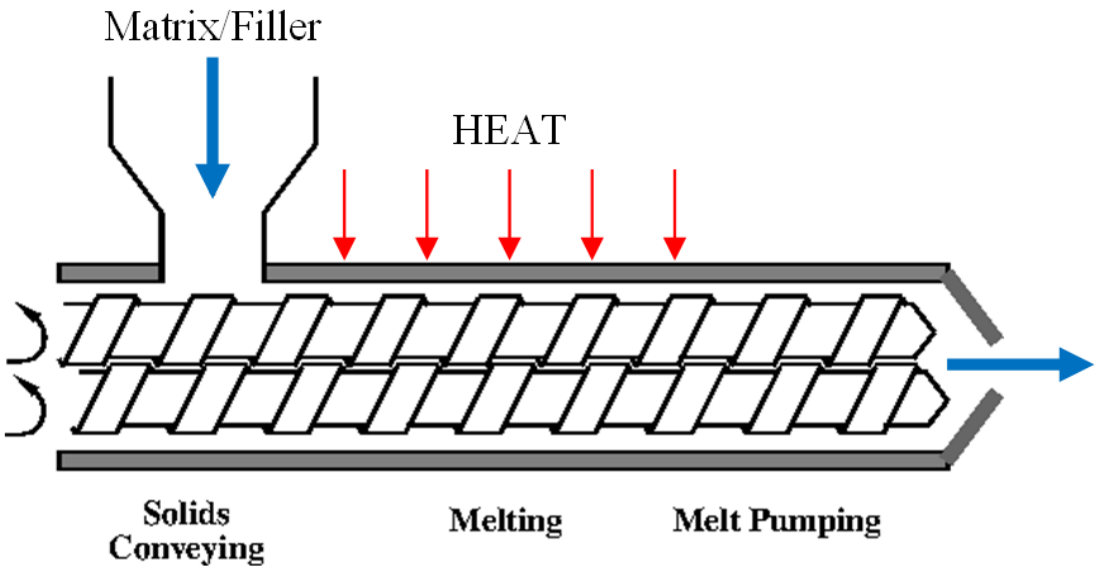

Figure 7. Twin Screw Extruder (TSE) [48].

Bucknell University's TSE instrument is a KrausMaffei Berstorff ZE-25A UTX: a co-rotational, intermeshing twin-screw extruder (Figure 8). The nominal length, L, of the

screw element designs are 850 mm while the diameters are 25 mm, yielding an L/D ratio of is 34. The barrel is divided into multiple zones as shown in Figure 9. Five of the six barrel zones are individually temperature controlled; in Figure 9, these are zones 2-6.

Figure 8. Bucknell University TSE/SSSP (KrausMaffei Berstorff ZE-25A UTX) [21].

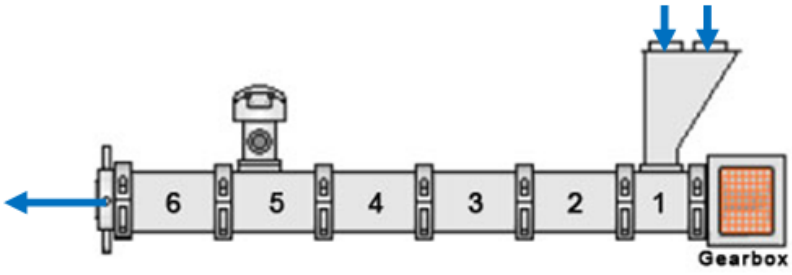

Figure 9. TSE/SSSP Zone Layout [38]. The blue arrows indicate material flow; arrows above the hopper, located on the right side of the image, indicate the material feed, while the arrow emerging from the extruder, located on the left side of the image, indicates outflow of extruded polymer.

Several auxiliary machines were used to feed ingredients into the TSE. The polymer matrix was supplied using a Brabender DS28-10 Pellet Feeder (Figure 10). The feeder operates by rotating an auger at a constant rate and pushing polymer pellets down a barrel and into the TSE feeding zone. The rotational speed of the auger can be modified to match the desired material mass flow rate, measured in grams per hour. The filler is supplied to the TSE using a Brabender DDSR12-1 feeder, shown in Figure 11. This feeder has smaller diameter twin-screw augers and is designed for powder feeding.

Figure 10. Brabender DS28-10 pellet feeder.

Figure 11. Brabender DDSR12-1 twin-screw stirring feeder.

3.2.2 Solid-State Shear Pulverization (SSSP)

Solid-state shear pulverization (SSSP) is a continuous and industrially-scalable solid-state processing method. An SSSP instrument is merely a modified TSE instrument. The barrel is cooled to keep the polymer matrix and filler well below their melting and softening temperatures by way of a re-circulating coolant maintained at -11 °C. SSSP employs four types of screw elements, shown in Figure 12, positioned on twin-screws that rotate inside the barrel. The specially designed screws (Figure 13) impart high shear forces which fracture the polymeric matrix, leading to pulverization. This process results in a fine powder. The nanofillers are added to the SSSP with the filler and the shearing action causes the fillers to intimately mix into the matrix phase.

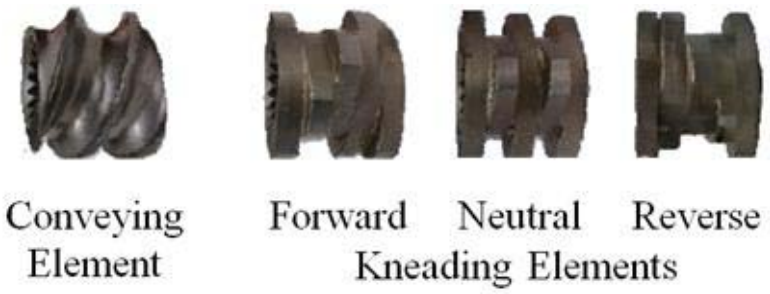

Figure 12. Image of basic screw element types available for screw design [21].

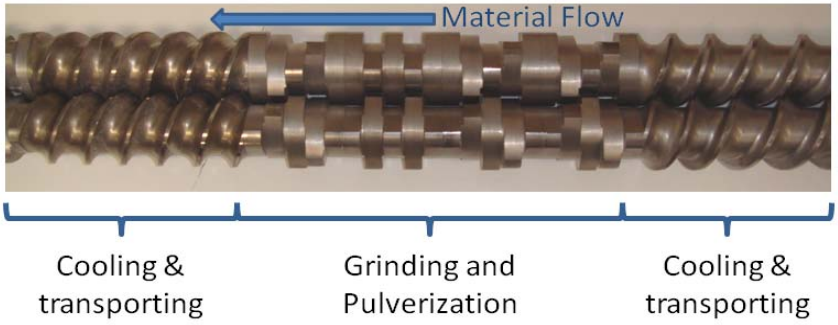

Figure 13. Twin screws for TSE/SSSP.

Bucknell University's SSSP instrument is a KrausMaffei Berstorff ZE-25A UTX and is described earlier (Figure 8). The nominal length of the screws element designs are 875 mm while the L/D ratio is 35 (D = 25 mm). The length difference between SSSP (875 mm) and TSE (850 mm) modes comes from an additional element used to move powder from the apparatus during solid-state operation [38].

When operating in the SSSP mode, barrel zones 2-6 are chilled by re-circulating coolant. Coolant, which is an ethylene glycol/water solution, is supplied by a Budzar Industries BWA-AC-10 water chiller. The polymer matrix and filler were supplied to the SSSP by the same feeders described in TSE operation.

3.2.3 SSSP-Single Screw Extrusion (SSE)

Solid-state shear pulverization followed by single screw extrusion (SSE) was the third processing technique examined in this project. Samples were first processed using KrausMaffei Berstorff ZE-25A UTX in SSSP mode, and subsequently were melt-mixed using a single screw extruder. Similarly to TSE, SSE is a continuous and industrially-applicable processing method in which the barrel is heated using electric heaters to allow the polymer matrix to melt. The difference between a SSE and TSE is that SSE only uses one screw to transport the molten polymer down the barrel; there is no kneading effect, only shear forces along the interior of the barrel.

The SSE is a Killian KLB-075 Bench Model Extruder (L = 45.6 cm, D = 1.9 cm, L/D = 24), and is shown in Figure 14. Materials, stored in a hopper, are gravity fed into

the barrel. Occasionally the hopper was prodded using a copper rod to break up clumps of feed material which was a SSSP powder.

Figure 14. Killian KLB-075 bench model single screw extruder.

3.3 Sample Preparation

Following processing, samples are an inconsistent strand shape (TSE/SSE) or a powder (SSSP). In order to prepare samples for analysis, they were compression molded into uniformly thick sheets using a Carver laboratory press seen in Figure 15. The platens on the press were set to 400 °F to press both HDPE and LLDPE. Samples and a spacing guide were loaded between aluminum plates protected by Mylar sheets, which prevented the sample from adhering to the plates. The press employs a hydraulic pump which raises and lowers the bottom platen to apply consistent pressure to molten polymer (Figure 16). Samples were left in the hot press for 5 minutes before being removed and placed on a counter for air cooling. SSSP-SSE samples were quenched immediately after removal to avoid the sample sticking to the Mylar sheets.

Figure 15. Carver laboratory press.

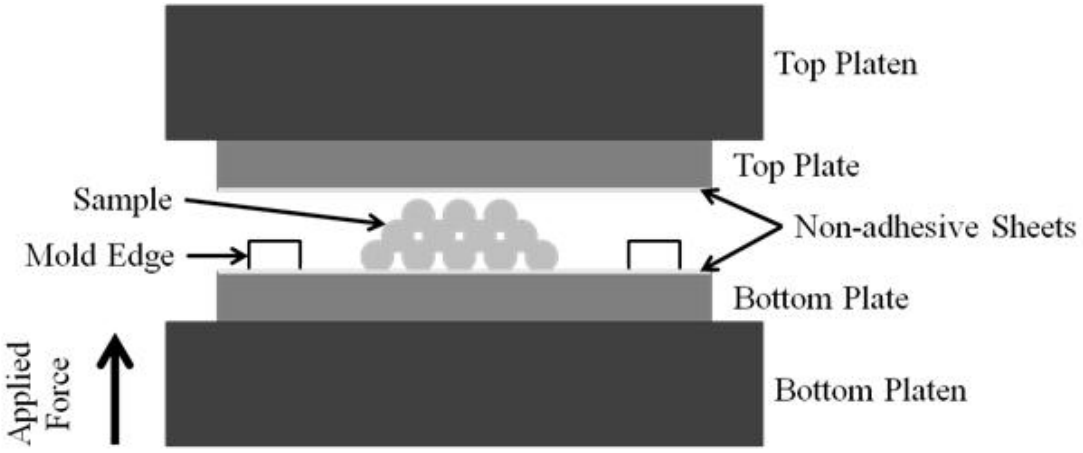

Figure 16. Schematic of setup during compression molding [21].

3.4 Property Testing

Multiple tests were employed to explore material and morphological characteristics of fabricated samples.

3.4.1 Thermogravemetric Analysis (TGA)

High temperature behavior of the processed specimens was examined using thermogravemetric analysis (TGA). A sample is placed on a small balance which is heated at a constant rate to temperatures exceeding the degradation temperature of the polymer. The polymeric material decomposes and become gaseous upon heating, and the weight loss (%) is recorded. By plotting residual mass versus temperature, a thermal degradation profile of a material can be analyzed. This not only gives insight to the high-temperature behavior of the PNC but also shows the actual weight percent of filler in the sample, as the filler remains in the pan without decomposing.

A TA Instruments Q600 was used. Each run filled an alumina ceramic pan with 10-20 mg of sample material which was then placed, along with a reference pan, onto the balance arms in the Q600. Runs consisted of a 10 ºC/min ramp from 30-600 ºC. Data were analyzed using the TA Thermal Analysis software. Degradation temperature was calculated by determining the corresponding temperature at 5% component mass loss [13].

3.4.2 Differential Scanning Calorimetry (DSC)

Differential scanning calorimetry (DSC) is used to precisely measure the heat flux in and out of sample for a range of temperatures, and detect phase transitions. DSC is capable of determining the glass transition temperature (T_g), melt temperature (T_m), and crystallization temperature (T_c) of polymeric samples. DSC uses a programmable heat profile to heat or cool a sample material within a sealed pan at a constant rate and

measures the heat flux response. DSC can also conduct isothermal runs to monitor the heat flux during an isothermal hold.

A TA Instruments Q1000 was used for DSC. Samples of 10-15 mg were placed in hermetic aluminum pans. An empty pan was used as a reference. Test runs consisted of 10ºC/min Heat/Cool/Heat cycles. Data were analyzed using the TA Universal Analysis software package.

We employ isothermal mode DSC as a way of measuring the level of filler dispersion within the matrix phase. Dispersion is the degree to which the filler is spread evenly around the matrix; more dispersion yields more uniform material behavior. Higher levels of dispersion are visible through faster and more complete crystal growth as dispersed fillers act as nucleation sites. Test runs consisted of 10ºC/min heating to 180 ºC, then jumping to 126.5 ºC (HDPE) or 123 ºC (LLDPE) and maintaining the temperature for 3 hours.

3.4.3 Tensile Testing

Tensile testing measures the mechanical properties of a sample, including breaking strain, elastic modulus (Young's modulus) and yield strength. A specimen is deformed to fracture with a gradually increasing tensile strain (i.e. stretching) that is applied uniaxially along the long axis of a specimen [49]. The breaking strain of a material is the elongation at which the material fractures entirely. Elastic modulus is a measure of material stiffness and is defined by the slope of the stress-strain curve during elastic deformation. Yield strength is the stress required to get to a yield point—an

irreversible transition from elastic to plastic mechanical behavior. It is defined as the maximum strength prior to extended plastic deformation, or permanent deformation.

A Tinius Olsen H5K-S Universal Tester is equipped with a 1000 N load cell. Dogbone testing samples cut from pressed polymer sheets using a Dewes-Gumbs manual expulsion press (ASTM D1708). Samples were tested at an extension rate of 0.5 in/min until failure and raw force vs. extension data were exported for further analysis [38]. An in-house software program was used to collect force versus elongation data, while a separate MATLAB program was used to analyze the collected data and determine breaking strain, elastic modulus (MPa) and yield strength (MPa). Force and extension is automatically converted to stress and strain by entering the sample dimensions. Yield strength and breaking strain are calculated, while elastic modulus is found by finding the slope of a line connecting two points in the linear elastic regime [38].

3.4.4 Gas Barrier Properties

Permeability meters are used to measure the gas-barrier properties of the PNC sample. In a permeability measurement, the sample is placed between two pressurized chambers, one with a high concentration of the permeant gas and the other with zero concentration. The diffusion of the permeant is monitored over time, until steady state is reached.

The samples are placed in-between two chambers of equal pressure, one with 100% oxygen gas, and the other with a hydrogen and nitrogen mixture, and the MOCON Permeability System software measures the steady state flux of oxygen (permeability, or

permeation coefficient) through the sample (Figure 17). Oxygen permeability, in standard units of $[(cm^3)(mil)]/[(m^2)(24hrs)(atm)]$, was recorded for analysis.

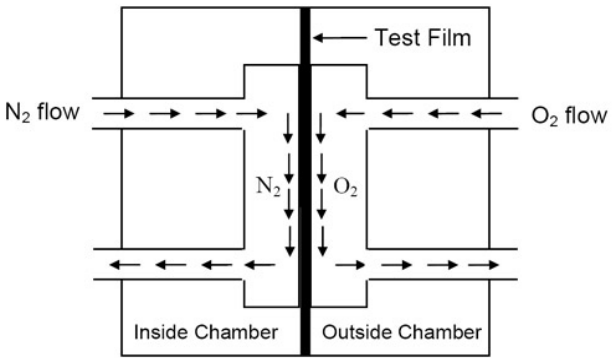

Figure 17. Schematic of oxygen permeation testing equipment. The trimmed, flat-sheet sample is placed in the center, and oxygen is allowed to permeate towards the nitrogen environment [50].

3.4.5 X-Ray Diffraction (XRD)

X-Ray Diffraction (XRD) is a technique employed to probe the crystalline structure of a material [51, 52], and is used to measure the degree of exfoliation of the nanoscale filler in the polymer matrix. It is a morphology probing technique as opposed to a property measurement technique. Exfoliation refers to the amount of separation that exists between the sheets of the filler. In the case of polymer nanocomposite materials, XRD is able to characterize both the matrix, if the polymer is semi-crystalline, and the filler, if the structure consists of repeated units on the nanometer scale [50].

Figure 18 shows that the incident X-ray beams are directed onto the surface of a sample and a detector opposite the beam source records the intensity of X-rays diffracted by the sample. The beam source and detector move at a constant rate during testing, changing the incident angle of X-rays relative to the sample. Ordered crystal structures

of the sample material produce constructive and destructive interference of X-rays depending on the incident angle of the beam [21]. XRD measures the spacing between sheets of atoms in the crystal using Bragg's Law:

$$n \cdot \lambda = 2 \cdot d \cdot \sin(\theta)$$

Where n refers to the degree (in this case 1), λ is the X-ray wavelength, d is the spacing between atomic sheets, and θ is the incident angle. Angles are traditionally reported as 2θ as both the X-ray source and X-ray detector move θ measured compared to the sample. At a specific wavelength and angle, the spacing between sheets of atoms is found. High linear intensity values indicate that at a certain 2θ the detector opposite the beam recorded a high intensity of X-rays diffracted by the sample. This corresponds to a higher number of clay sheets spaced at a particular d.

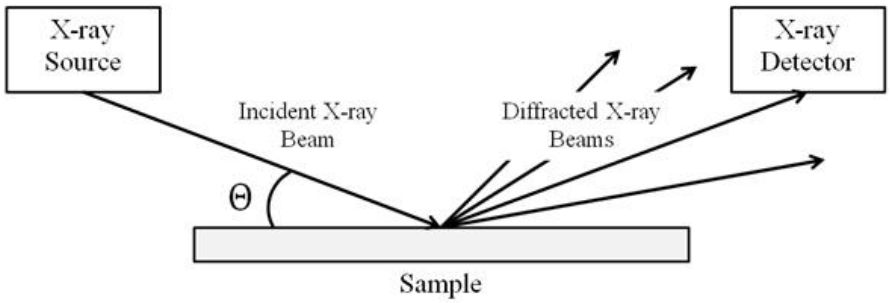

Figure 18. Schematic of XRD [21].

Samples of approximately 1" x 1" x 1/16" were cut from pressed sheets. A PANalytical (Philips) X'Pert Pro Multi-Purpose Diffractometer (MPD) System with a ceramic broad-focus Cu X-Ray Tube was used for XRD tests. X-rays at 45 kV and 40 mA were emitted through 1/16° fixed slits. PANalytical (Philips) X'Pert Data Collector and X'Pert HighScore Software were used to analyze the collected data. The

recorded intensity of X-rays off the sample corresponds to the degree of stacked nanofiller in the polymer matrix. A higher intensity at a specific angle indicated poor exfoliation.

4. Results

The following chapter shows the data collected during this study. For the remainder of this thesis, the following nomenclature will be used to refer to polymer and PNC samples: polymer matrix will be designated by either an H (HDPE 7320) or an L (LLDPE 2027), filler type will be designated by N (neat—no filler), O (organo-clay), or P (pristine clay), processing type will be designated by E (twin-screw extrusion), Sh (harsh solid-state shear pulverization), Sm (mild solid-state shear pulverization), or Se (mild solid-state shear pulverization followed by single-screw extrusion). Filler loading percent is shown in parentheses. Table 2 summarizes the samples processed for this thesis.

All filled PNCs were designed to contain 5 wt% clay as the target filler content; the observed loading percents, determined via TGA by measuring the residual mass in reference to the original mass of sample, shown in Table 2 do not match the target loading percentages. When the samples were processed, both the polymer and filler feeders were calibrated several times. In practice, it is not easy to control the loading of clay as demonstrated by the inconsistencies in loading.

XRD was employed to explore the morphology of the fabricated PNCs. Figures 19-22 show the XRD diffractograms for HO, HP, LO, and LP PNCs, respectively.

Table 2. Samples fabricated during study with observed clay weight percents.

Code	Polymer Matrix	Filler	Processing Technique	Target wt%	Observed wt%
HN(0.0)	HDPE 7320	Neat		0	0.0
HOE(2.8)	HDPE 7320	Organo	TSE	5	2.8
HOSh(1.9)	HDPE 7320	Organo	Harsh SSSP	5	1.9
HOSm(4.8)	HDPE 7320	Organo	Mild SSSP	5	4.8
HOSe(6.7)	HDPE 7320	Organo	Mild SSSP - SSE	5	6.7
HPE(4.8)	HDPE 7320	Pristine	TSE	5	4.8
HPSh(7.0)	HDPE 7320	Pristine	Harsh SSSP	5	7.0
HPSm(3.9)	HDPE 7320	Pristine	Mild SSSP	5	3.9
HPSe(7.0)	HDPE 7320	Pristine	Mild SSSP - SSE	5	7.0
LN(0.0)	LLDPE 2027	Neat		0	0.0
LOE(0.8)	LLDPE 2027	Organo	TSE	5	0.8
LOSh(3.8)	LLDPE 2027	Organo	Harsh SSSP	5	3.8
LOSm(8.6)	LLDPE 2027	Organo	Mild SSSP	5	8.6
LOSe(5.0)	LLDPE 2027	Organo	Mild SSSP - SSE	5	5.0
LPE(4.2)	LLDPE 2027	Pristine	TSE	5	4.2
LPSh(5.8)	LLDPE 2027	Pristine	Harsh SSSP	5	5.8
LPSm(4.6)	LLDPE 2027	Pristine	Mild SSSP	5	4.6
LPSe(6.1)	LLDPE 2027	Pristine	Mild SSSP - SSE	5	6.1

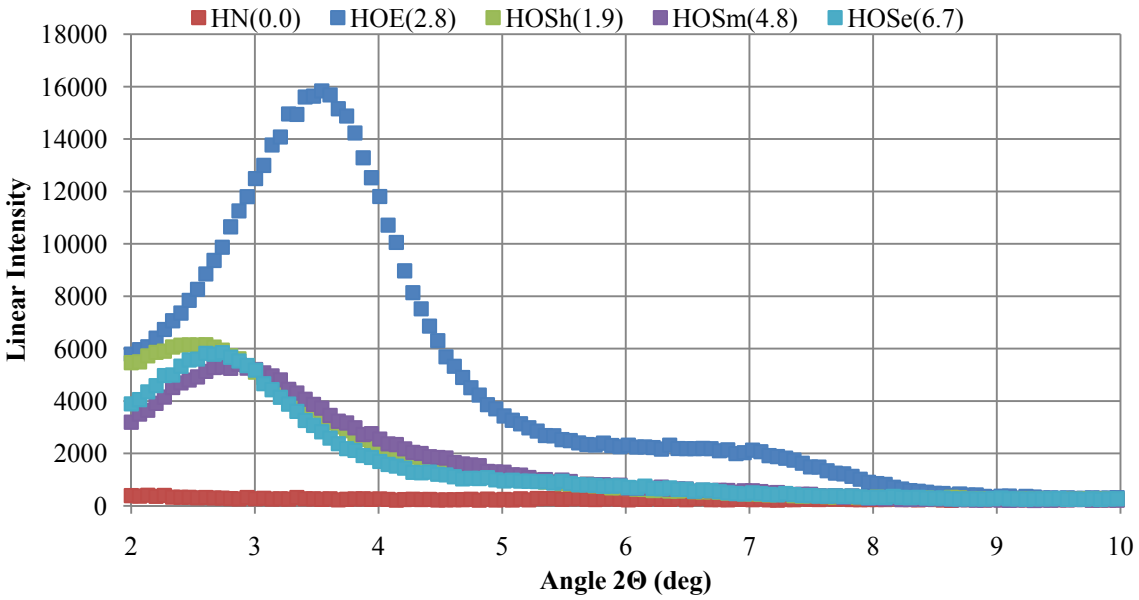

Figure 19. XRD Diffractogram for HO polymer samples, with the organo-clay peak visible at 2θ ≈ 2.5-3.5°.

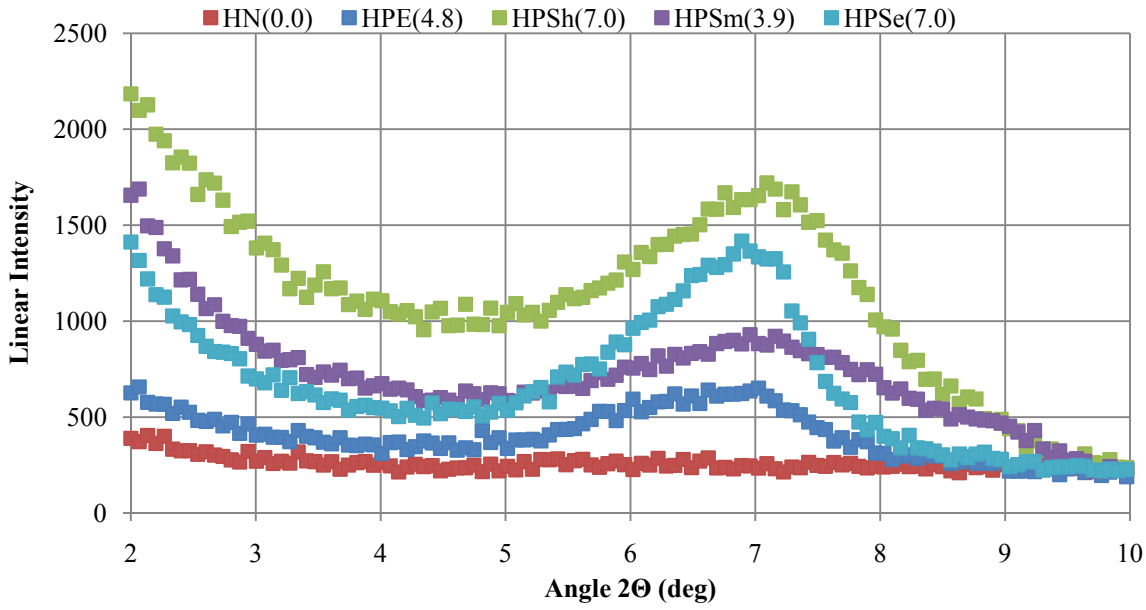

Figure 20. XRD Diffractogram for HP polymer samples, with the pristine clay peak visible at 2θ ≈ 7°.

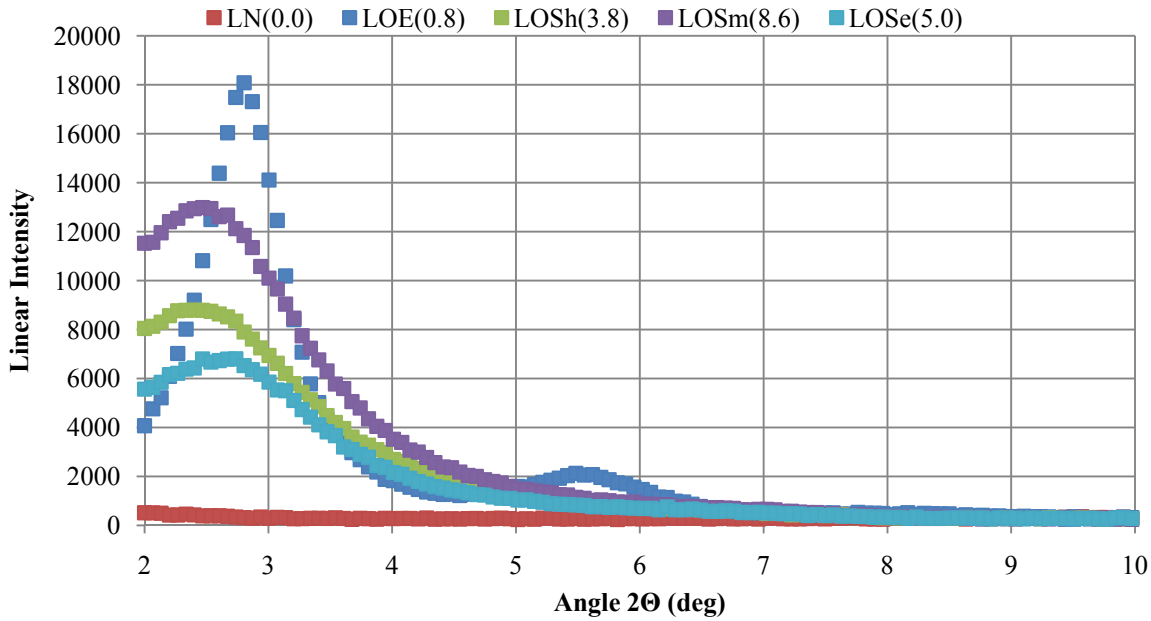

Figure 21. XRD Diffractogram for LO polymer samples, with the organo-clay peak visible at 2θ ≈ 2.5-3°.

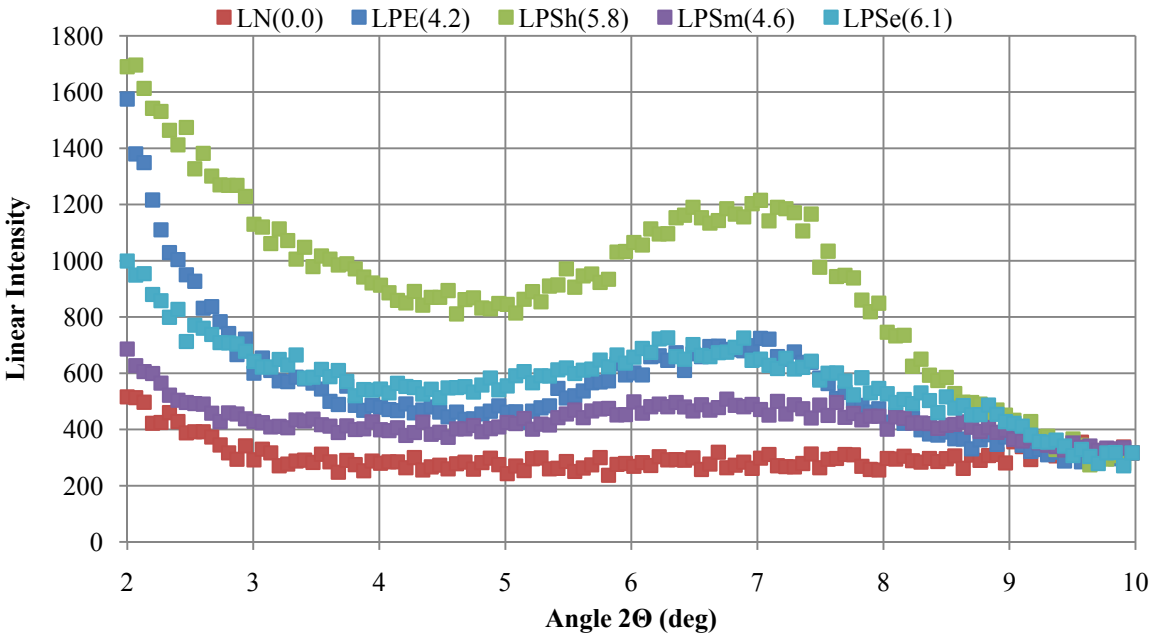

Figure 22. XRD Diffractogram for LP polymer samples, with the pristine clay peak visible at 2θ ≈ 7°.

An apparent shift of the clay peaks to a lower 2θ for SSSP-processing compared to extrusion in Figures 19 and 21 indicates that there is intercalation. Intercalation is when the polymer chains penetrate between the silicate sheets of clay particles via some external treatment or processing method and thus physically separating the clay inter-sheet spacing. Peaks also shifted downwards for SSSP-processing compared to extrusion for organo-clay samples, indicating that SSSP achieved higher levels of exfoliation than extrusion. This trend is not seen in pristine-clay systems.

DSC also investigated the morphological characteristics of the samples. DSC analyses, whose results are summarized in Table 3, focused on dispersion by measuring crystal growth. This is indicative of the number of nucleation sites within the polymer matrix. Figure 23 shows a sample Heat-Cool-Heat curve which is used to determine the onset crystallization temperature, melting temperature, and the amount of polymer crystals (termed crystallization), which is measured via latent heat of melting in units of joules per gram. There is a subtle improvement in crystallization of SSSP samples, especially in HOSm, compared to extruded and neat samples. For an isothermal crystallization process, crystallization half-time—the time required for half of the sample to crystallize—was calculated for each sample. The area under the heat flux curve during the isothermal hold represents the crystallinity of the PNC. From this area, the percent crystallization at a given time was determined.

Table 3. DSC data for crystallization, crystallization half-time, and onset crystallization temperature.

Code	Peak Melting Temperature (°C)	$\Delta H_{Melting}$ (J/g) (% Compared to Neat)	Onset Crystallization Temperature (°C)	Crystallization Half-Time (min) (% Compared to Neat)
HN(0.0)	134	215	122	32
HOE(2.8)	133	199 (-7%)	121	43 (-32%)
HOSh(1.9)	134	224 (4%)	122	40 (-24%)
HOSm(4.8)	139	189 (-12%)	121	42 (-29%)
HOSe(6.7)	133	196 (-9%)	121	33 (-3%)
HPE(4.8)	135	198 (-8%)	121	38 (-16%)
HPSh(7.0)	134	209 (-3%)	123	46 (-43%)
HPSm(3.9)	135	227 (6%)	122	39 (-20%)
HPSe(7.0)	136	157 (-27%)	121	35 (-9%)
LN(0.0)	128	189	115	75
LOE(0.8)	128	192 (2%)	116	40 (48%)
LOSh(3.8)	129	189 (0%)	117	35 (53%)
LOSm(8.6)	129	143 (-24%)	117	29 (62%)
LOSe(5.0)	129	171 (-10%)	117	29 (61%)
LPE(4.2)	129	170 (-10%)	116	41 (46%)
LPSh(5.8)	129	197 (4%)	121	20 (74%)
LPSm(4.6)	129	187 (-1%)	118	25 (66%)
LPSe(6.1)	129	160 (-15%)	118	27 (64%)

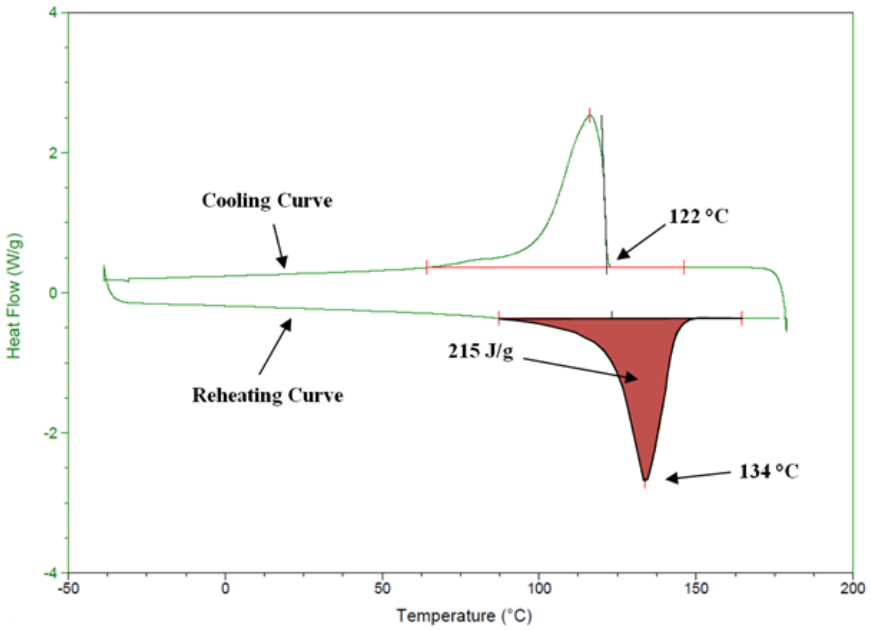

Figure 23. Heat-Cool-Heat DSC thermogram showing temperature vs. heat flow curve for HN. The top curve is the cooling curve while the bottom curve is the reheating curve. The peak melt temperature (134 °C) and onset crystallization temperature (122 °C) are shown by arrows. The latent heat of melting, which corresponds to PE crystallinity, is shown by the shaded red area (215 J/g).

Figure 24 displays the onset crystallization temperatures graphically and demonstrates that the addition of fillers in HDPE 7320 samples generally decreased onset crystallization temperature compared to HN whereas fillers always increased onset crystallization temperature of LLDPE 2027 samples compared to LN. Of note is LPSh, which has a substantially higher value than LN.

Table 4 shows that the degree of polymer crystallinity varied from sample to sample. As for isothermal results, for HDPE samples, crystallization half-time did not improve with the addition of a filler; however, LLDPE samples saw a drastic reduction in crystallization half-time indicating the presence of more nucleation sites in the polymer matrix compared to LN.

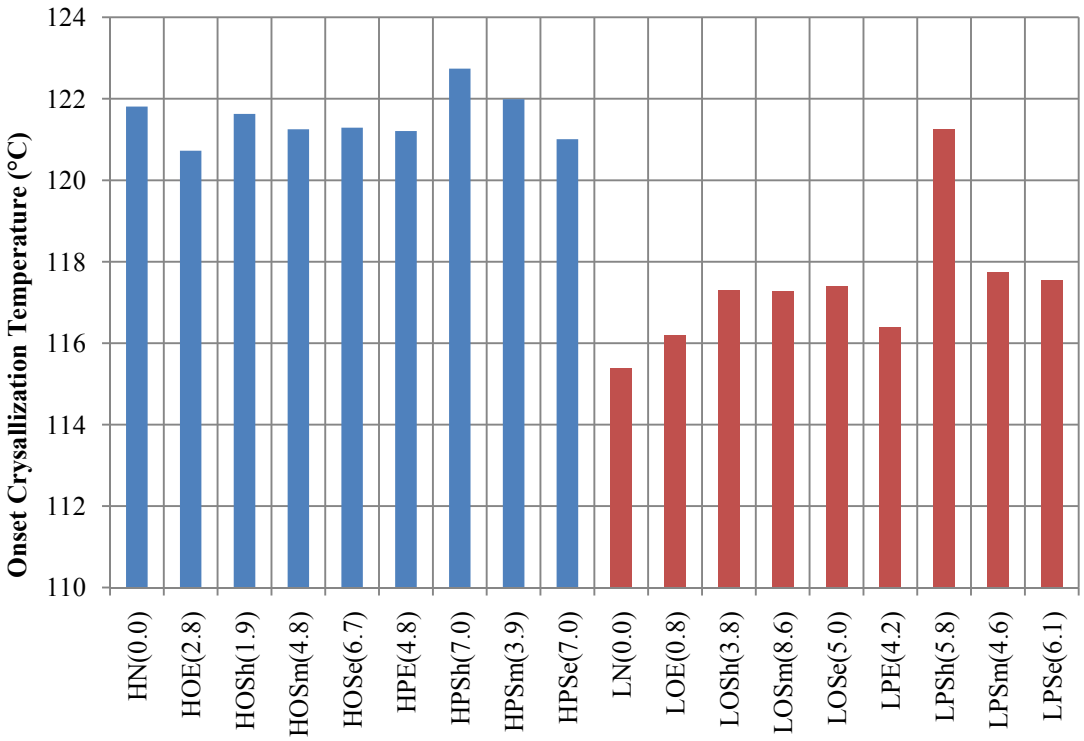

Figure 24. Onset crystallization temperatures (°C) for HDPE 7320 and LLDPE 2027 based polymers.

Thermal degradation temperatures, summarized in Table 4, were determined using TGA, measured as the temperature at which 5 wt% of the sample had disintegrated and burned off. Table 4 summarizes these findings. Reduction in thermal stability at high temperatures for both HDPE and LLDPE compared to neat samples, shown in Table 4, is unexpected as the addition of high-performance fillers typically improves the high-temperature performance of PNCs.

Mechanical characterization of the samples was performed using tensile testing. Yield strength, elastic modulus, and breaking strain are shown in Figures 25-27, respectively.

Table 4. Thermal degradation temperatures of polymer samples.

Code	Degradation Temperature (°C) (% Reduction in Temperature Compared to HN)	Code	Degradation Temperature (°C) (% Reduction in Temperature Compared to LN)
HN	447	LN	453
HOE	439 (-2%)	LOE	444 (-2%)
HOSh	440 (-2%)	LOSh	441 (-3%)
HOSm	435 (-3%)	LOSm	434 (-4%)
HOSe	391 (-13%)	LOSe	396 (-13%)
HPE	383 (-14%)	LPE	429 (-5%)
HPSh	444 (-1%)	LPSh	435 (-4%)
HPSm	413 (-8%)	LPSm	430 (-5%)
HPSe	407 (-9%)	LPSe	414 (-9%)

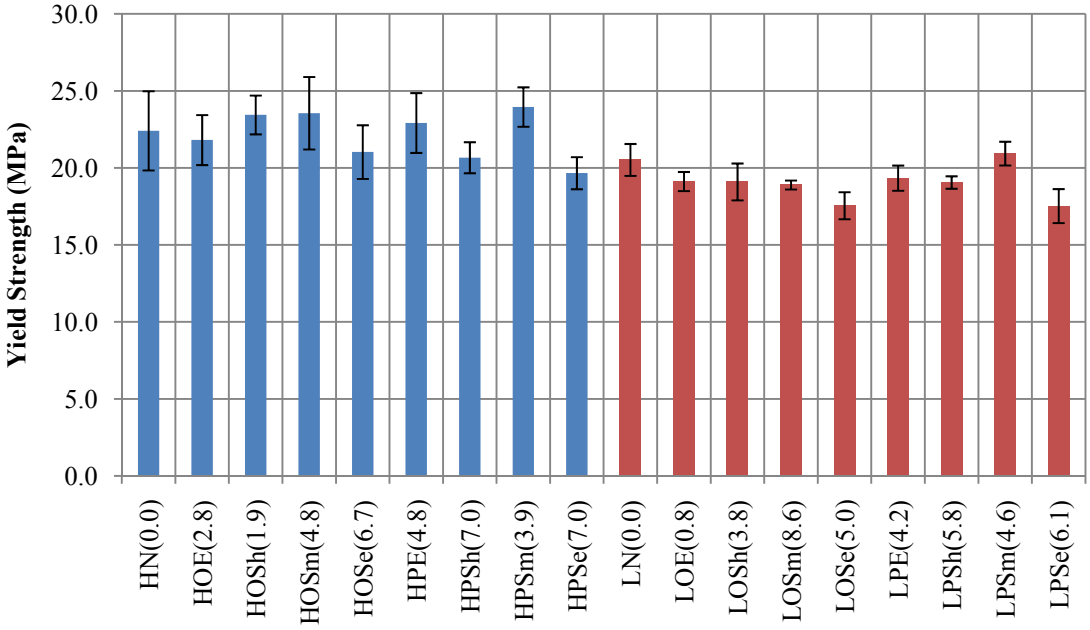

Figure 25. Yield strength (MPa) of samples, with HDPE samples shown in blue and LLDPE samples shown in red.

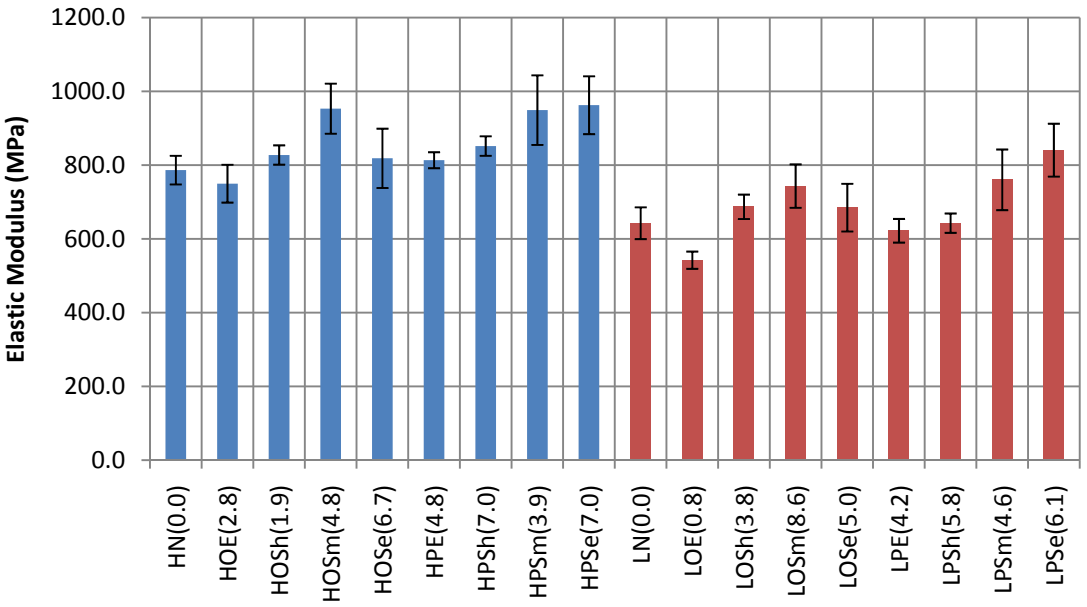

Figure 26. Elastic modulus (MPa), with HDPE samples shown in blue and LLDPE samples shown in red.

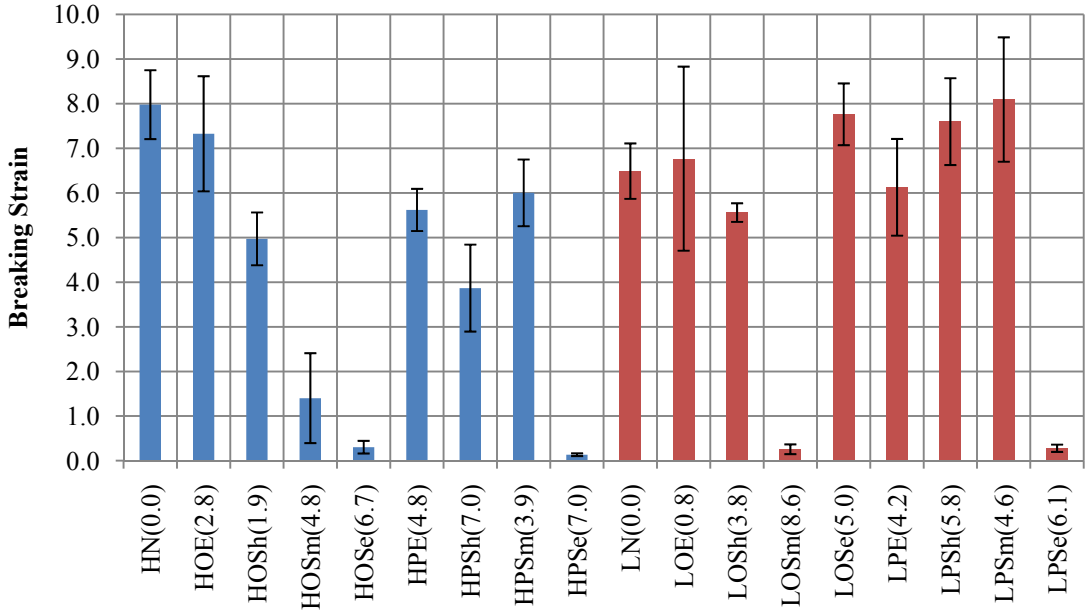

Figure 27. Breaking strain, with HDPE samples shown in blue and LLDPE samples shown in red.

Figure 26 demonstrates that the addition of fillers to a polymer matrix generally increases modulus, particularly in HDPE samples. HDPE is more mechanically robust than LLDPE due to the polymer material morphology; denser packing of polymer strands and a higher crystallinity compared to LLDPE result in both stronger and stiffer materials. Furthermore, mild SSSP is capable of achieving stiffer samples compared to other processing techniques. Extreme reduction in ductility was observed in several samples, though there is no trend.

The gas barrier property results from oxygen permeation test are shown in Figure 28. Extrusion processing is generally the best for achieving superior gas barrier properties; however, it is still true that adding clay with SSSP moderately reduces permeation compared to neat samples, particularly for LLDPE samples.

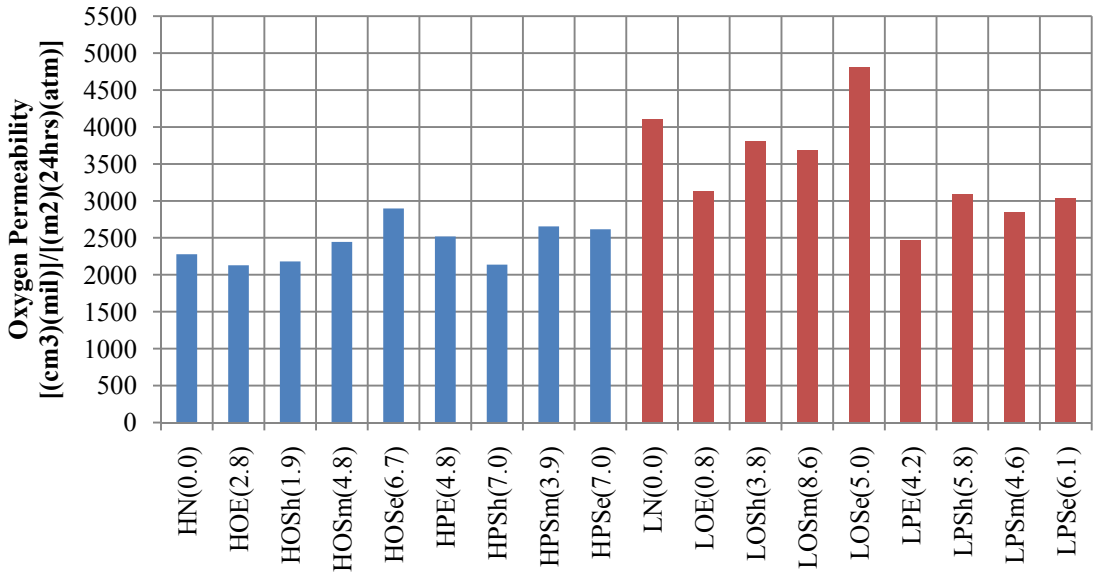

Figure 28. Oxygen permeability [(cm^3)(mil)]/[(m^2)(24hrs)(atm)] for the fabricated PNCs, with HDPE samples shown in blue and LLDPE samples shown in red. Lower values indicate better gas barrier properties.

5. Discussion

The goal of this thesis was to understand how processing parameters affect the morphology and physical properties of the most basic, fundamental PNC system, namely PE with clay. As the data presented in the Results section depend on numerous variables such as polymer type, filler type, and processing conditions, we focus on a series of binary comparisons and provide discussions for each. In this way, parameter effects can be isolated. This portion of the thesis presents the following comparisons: HDPE vs. LLDPE, pristine clay vs. organo-clay, extrusion (heated) vs. SSSP (cooled), harsh SSSP vs. mild SSSP, and post-SSSP SSE vs. SSSP without subsequent processing.

5.1 HDPE vs. LLDPE

The difference in molecular structure of HDPE and LLDPE described earlier leads to significant practical differences such as density, melting temperature and mechanical strength. Table 3 in Chapter 4 shows that HN has higher crystallinity and higher melting and crystallization temperatures than LN.

Polymer morphological differences affect the material performance, as evident in Figure 25, which shows yield strength, and Figure 26, elastic modulus. In both instances, values for HDPE PNCs are slightly higher than LLDPE PNCs indicating that the former is both stronger and stiffer. This is to be expected as the polymer chains are capable of packing more closely in HDPE. The chemical structure is equivalent for both polymers; however, in HDPE denser packing and the presence of more, larger crystals make the polymer stronger and less ductile. This difference in polymer crystal structure also

affects gas barrier properties; HDPE is more densely packed and therefore should demonstrate superior barrier properties. Figure 28 indicates lower permeability levels for HDPE compared to LLDPE.

As the molecular structure of HDPE and LLDPE leads to considerable practical differences, it follows that the physical properties of the two polyethylenes when filled with clay would most likely be distinctly different in a similar fashion as well. The addition of a filler to a polymer matrix generally improves, or at least retains, material strength and stiffness. Clay inclusion traditionally helps the polymer nucleate more crystals which contribute to stiffness, strength, and permeation barrier properties.

Several tests indicated that HDPE properties worsened in PNCs compared to the neat form. Crystallization half-times increased (crystallization is slower) for HDPE samples when a filler was added. However, for LLDPE samples, crystallization half-time decreased 60% on average regardless of processing parameters (Table 3). This is because fillers act as a nucleating agent and promote crystal growth in the polymer matrix. Degradation temperature was shown not to change considerably; most samples saw a modest reduction in degradation temperature of only 2-8% compared to neat polymers (Table 4). Both crystallization half time and degradation studies were based on only one sample, and therefore more data are needed for to demonstrate statistical significance. Fillers yielded stiffer PNCs for both HDPE and LLDPE as demonstrated by Figure 26 without appreciably lowering the yield strength. Breaking strain seemed to vary considerably for both HDPE and LLDPE, showing both improved and deteriorated values

independent of filler type in Figure 27. LLDPE gas barrier properties were improved due to inclusion of fillers (Figure 28), but the same trend was not seen in HDPE samples. In general, it was found that material properties for LLDPE PNC samples improved considerably more than in HDPE PNC samples when either clay filler was added.

The results of this thesis indicate that clay fillers are more effective with LLDPE than HDPE. In highly crystalline structures such as HDPE, the inclusion of fillers does not enhance material properties considerably. Filler particles in already highly crystalline polymers might actually act as hinderers of crystal growth and prevent polymer strands from packing as closely as in a neat matrix. In lower crystallinity systems, clay particles help increase nucleation sites and thus promote faster crystallization, yielding larger crystals.

When one examines the results in more depth, it becomes apparent that the clay type affected HDPE and LLDPE differently, and it is worth focusing on the clay type as a binary comparison. This analysis is performed in the following section.

5.2 Pristine Clay vs. Organo-Clay

Researchers in the PNC community seem to focus on organo-clay because it is chemically more compatible with polymeric systems [53-58], especially those made of polyethylene.

As both pristine and organo-clay systems were examined in this study, comparisons can be made between clay type, holding matrix and processing conditions

constant. Figure 28 shows that pristine clay yields 25% lower permeation values on average than organo-clay in an LLDPE matrix. Direct comparison of LPSh and LOSh demonstrates a 4 °C increase of onset crystallization temperature and a 44% shorter crystallization half-time (Table 3). Figure 27 suggests that pristine samples were able to retain ductility better than comparable organo-clay samples for LPSh, LPSm, and HPSm. Comparing HO samples to HP samples, there was little difference in most characterization tests; there was no major difference in crystallinity, onset crystallization temperature, melt temperature, or crystallization half-time, nor was there a discernable difference in mechanical properties. Degradation temperatures across the two samples are inconclusive. Furthermore, pure organo-clay was shown to decompose at high temperatures during TGA tests; it was found that organo-clay begins to degrade at 260 °C (5% degradation) and that approximately 44% of added organo-clay thermally degrades at 550 °C (Figure 29).

One finding of this thesis, therefore, is that organo-clay is not significantly better suited for SSSP processing than pristine clay; in fact, pristine clay appeared to be more a compatible filler with LLDPE than organo-clay. This finding seems to refute the belief commonly held by PNC researchers who focus on traditional processing techniques.

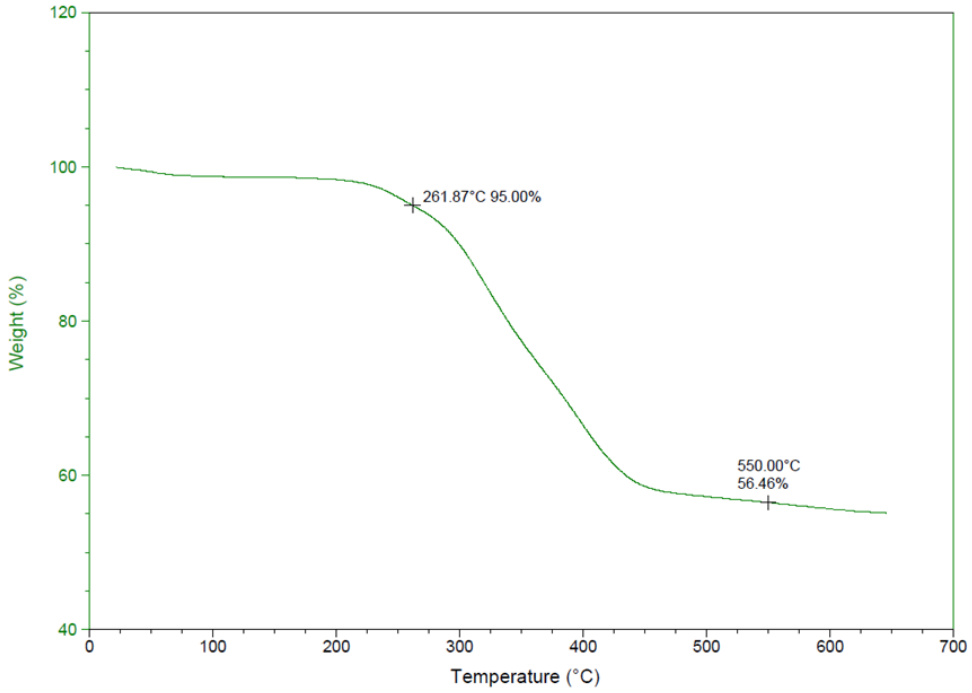

Figure 29. Degradation of organo-clay filler using TGA. Clay degradation begins at 260 °C. 44% of clay degrades by 550 °C.

Figures 19-22 show very different XRD diffractograms for pristine and organo-clay-filled polymers. Figures 19 and 21, HO and LO, respectively, show very high intensity peaks compared to the neat state whereas in Figures 20 and 22, the linear intensity is considerably lower. Furthermore, the sharp nature of the peaks for organo-clay samples compared to pristine-clay samples as indicative of the small degree of variability in the clay spacing. Pristine clay samples only experience a lowering of peaks which equates to different levels of exfoliation. Organo-clay samples saw a lowering height and additional shifting along the x-axis, which is indicative of exfoliation and intercalation.

Pristine clay is natural—it has not been modified with organic additives— and therefore seems more conducive to harsh mechanical processing via SSSP. Conversely,

organic molecules, which are weaker and lower melting, are present in organo-clays. SSSP processing on less thermally and mechanically robust organo-clay may lead to mechanochemical degradation of the clay. The physical and mechanical energy of mixing must be an important factor in SSSP, and therefore we will next compare the effect of sold-state shearing vs. melt-mix processing.

5.3 Heated Extrusion vs. SSSP

Chapter 2 discussed the drawbacks of heated extrusion and promoted SSSP as a superior processing technology. Melt mixing produces a high temperature environment that encourages this re-agglomeration of filler entities while SSSP avoids this by processing well below the melt/glass temperatures of the polymers or fillers. DSC and XRD can be used to measure the extent of dispersion and exfoliation, respectively, in an attempt to compare the two processing techniques.

In HDPE series, clay addition worsens the crystallization rate overall. On the other hand, crystallization rates for LLDPE samples were shorter for SSSP-ed samples than extruded samples: LOSm<LOSh<LOE<LN and LPSh<LPSm<LPE<LN (Table 3). Faster crystallization could be due to an increased number of polymer crystal nucleation sites, and this can lead to higher levels of filler dispersion in the matrix phase. Further supporting this claim are the increases in onset crystallization temperatures for SSSP-ed samples compared to extruded samples; PNCs with more nucleation sites will be able to crystallize at higher temperatures. LO samples saw an increase of about 1 °C for SSSP

compared to TSE while LP saw an increase of 1-5 °C. There was no change in melt temperature with varying processing methods.

Figures 19 and 21 demonstrate higher levels of exfoliation were achieved in HOSh and HOSm compared to HOE, and similarly in LOSh and LOSm compared to LOE. Figure 22 shows that while LPSh was not an improvement from LPE, LPSm was. Furthermore, HPSm was not considerably worse than HPE. These findings suggest that SSSP is capable of higher levels of exfoliation of the filler sheets compared to extrusion.

While SSSP processing was shown to yield higher levels of dispersion and exfoliation, similar improvements were not as clearly demonstrated using mechanical analysis. Comparison of the yield strengths and breaking strains of LOE and LOSh indicates that there is practically no improvement ($t=0.036$, degrees of freedom (DF) = 2 and $t=1.16$, DF = 14, respectively, both with 95% confidence). There was, however, statistical improvement in elastic modulus ($t=6.45$, DF = 3, 95% confidence). Similarly, LOSm had a statistically significant improvement ($t=4.64$, DF = 8, 95% confidence) in elastic modulus.

5.4 Harsh SSSP vs. Mild SSSP

Chapter 3 discussed the various processing parameters that can be altered on Bucknell's SSSP instrument. Among those parameters is screw design; the degree of shear and compression in the SSSP can potentially change drastically depending on which screw elements (Figure 12) are used to construct the screws. Harsh screw design incorporates many kneading elements (some of which are reverse elements) which apply

compressive and shear forces on the polymer and filler. The mild screw design was constructed out of only a few forward and neutral kneading elements. This meant that the materials were kept at a lower temperature compared to the harsh design, as friction during pulverization increases the temperature inside the barrel.

There was no apparent trend in the crystallinity in harsh samples compared to mild samples. The crystallization half-time of HO was comparable for harsh and mild conditions, 29 % longer for LPSm than LPSh, 17% shorter HOSm than HOSh, and 18% shorter for LOSm compared to LOSh. Onset crystallization temperature was 1 °C higher for HPSh and 4 °C higher for LPSh compared to mild samples; HO and LO samples were virtually equivalent as shown in Table 3. Melt temperature was also unchanged. The degradation temperature of HPSm was 7% lower than HPSh but HO, LO, and LP samples recorded little or no difference. Mechanical properties were widely variant. Elastic moduli were higher for mild samples compared to harsh (15% for HO, 11% for HP, 8% for LO, and 18% LP) per Figure 26. Breaking strain was 55% higher for HPSm compared to HPSh and 6% higher for LPSm compared to LPSh, but mild samples were 71% lower for HO and 95% lower for LO. Yield strength saw no difference between HO and LO samples, but mild was 16% higher for HP and 10% higher for LP. Further statistical analysis of mechanical property data is required before more definitive conclusions can be made. Permeability of mild processing was 12% higher in HO and 24% higher in HP samples, but 3% and 8% lower in LO and LP, respectively. Lower permeability values indicate better gas barrier properties.

Analysis indicates that there is a noticeable difference in the material properties of PNCs fabricated under harsh and mild SSSP conditions. Dispersion levels, measured via the degree of crystallinity, crystallization half-time, and onset crystallization temperature did not seem to be higher for one processing technique over the other. The same can be said about degradation temperature. XRD indicates higher levels of filler exfoliation, which would also increase tortuousity, for Sh compared to Sm in LO samples. Sm achieves better exfoliation in the other three polymer/filler combinations. Mechanical properties appeared to be appreciably better for mild SSSP than for harsh; materials were stiffer and stronger, though they did surrender some ductility. Harsh processing yielded enhanced gas barrier properties. Harsh processing can cause significant, potentially excessive, chain scission of the polymer, which can disrupt channels for gas particles, but at the same time, can harm mechanical properties as the polymer chains and crystalline structure are degraded.

5.5 Post-SSSP SSE vs. SSSP without Subsequent-Processing

As critics of SSSP question the expenditure of time and energy to maintain a low energy environment if the product of SSSP must be heated to make any consumer or industry goods, one goal of this study was to examine the effects of heated processing following SSSP.

Melt processing of mild SSSP samples (Se) negatively affected most of the material properties of the fabricated PNCs. Post-SSSP SSE had no effect on the onset crystallization temperature, the degree of crystallinity, or the crystallization half-time for

LO samples, thought it actually improved the crystallization half-times of HO and HP samples by 20% and 9%, respectively. However, in nearly every other instance, post-SSSP processing caused material properties to worsen. Degradation temperature decreased in HO samples by 10%, HP by 1.5%, LO by 9% and LP by 4% comparing Sm to Se processing. Yield strength decreased 11% for HO, 18% for HP, 7% for LO and 16% for LP, however further statistical analysis is warranted. Modulus and breaking strain saw more regression than progression, but had mixed impacts. Permeability increased by 19% for HO, 30% for LO and 7% for LP and decreased 1% for HP. XRD shows that while exfoliation was better in LOSe than in LOSm (Figure 21), Sm processing typically achieved superior levels of exfoliation than Se samples (Figures 19, 20 and 22).

These trends indicate appreciable deterioration of material properties and morphological characteristics of the PNCs. In contrast, Torkelson and Masuda's post-SSSP melt mixing of CNTs, discussed in Chapter 2, saw material property improvements when PNCs were fabricated via post-SSSP melt mixing; apparently this process was successful for CNTs but the same cannot be said for clays. Lower degradation temperatures indicate poorer high-temperature performance, which may be due to degradation of the polymer and filler during SSE. Reduction of yield strength and exfoliation further indicates that extrusion post solid-state pulverization partially undoes some of the processing achievements of SSSP. The lack of any serious or meaningful material improvements reiterates this fact.

6. Conclusions and Recommendations

Multiple processing parameters were investigated for the fabrication of polyethylene-clay PNCs. Numerous variables, including the type of polymer and filler and processing techniques, were adjusted over the course of this research, resulting in multi-faceted sets of data. Five binary comparisons were conducted in an attempt to isolate and analyze the effects of individual parameters. Several comparisons yielded notable conclusions which are discussed in this chapter along with recommendations for future work.

There was an obvious inconsistency in the filler loading in the fabricated samples processed by both TSE and SSSP. Even though we proceeded with care by calibrating both the polymer and filler feeders and took several test measurements, we still were unable to achieve uniform loading across polymer/filler combinations. We were not patient enough to watch filler percent before collecting. One recommendation would be to wait longer for the system to reach a steady-state output before collecting sample. Multiple rate measurements should be taken before collecting the sample. Composition could therefore be verified with more certainty and adjustments could be made should the output composition not match target values.

This study showed that inclusion of a filler was more beneficial to a less crystalline polymer than that with a high degree of crystallinity. It was found that LLDPE was more compatible with both organo- and pristine clay fillers. In fact, several tests indicated that HDPE properties worsened in PNCs compared to neat HDPE. Future

efforts should be directed at finding other PNC matrix materials which can be improved through the addition of a filler and SSSP processing. It is suggested that polymers with a low degree of crystallinity be examined first. Additionally, a study similar to the one performed by Wakabayashi et al. [12] should be performed in which the loading percentage of clay is varied holding processing technique and polymer matrix constant. This type of study could help verify or disprove the findings of this thesis based on the effects of filler loading on material properties for PE/clay systems.

One major finding of this thesis was that, contrary to popular sentiment [53-58], organo-clays are no better suited for SSSP processing of PNCs than pristine clay is. Multiple tests showed greater property enhancements in pristine clay samples compared to the respective organo-clay samples. These improvements were more visible in LLDPE samples than in HDPE samples which relates to the previous conclusion pertaining to filler compatibility; specifically, pristine clay appeared to be more a compatible filler with LLDPE than organo-clay. While the superiority of pristine clay over organo-clay was shown for PE based PNCs, the conclusion should be investigated with other polymer matrices. Polypropylene is a common polymer choice in PNC studies; therefore it is recommended that a similar study to this be conducted for PP/clay PNCs.

There is a noticeable difference in the material properties of PNCs fabricated under harsh and mild SSSP conditions. While harsh processing yielded enhanced permeability properties, mild processing yielded improved mechanical characteristics. Optimal screw design will ultimately depend on the polymer/filler combination being

processed as well as temperature and screw speed; however, further research should be conducted to isolate the effects of various screw configurations ranging from very mild to very harsh and low to high screw speed. In this way, SSSP would be better classified and tunable to specific processing requirements.

Several studies have demonstrated the supremacy of SSSP-processing compared to other techniques currently employed by industry, predominantly extrusion. Still to be answered about the SSSP is whether or not applying heat undoes the high levels of dispersion and exfoliation achieved with SSSP techniques. The application of heat subsequent to harsh SSSP conditions could also degrade the product. Extrusion following SSSP was shown to deteriorate material properties that had previously been improved via SSSP processing. This study only examined one processing speed for SSE and therefore this claim is not definitive across all extrusion residence times (time the sample spends in the extruder). Further study is needed to determine the effect of extrusion residence time on post-SSSP melt-mixed samples. Additionally, post-processing was only investigated for mild SSSP processing; the effects of post-processing on harsh SSSP should be explored.

7. References

[1] Brandrup, J. *Polymer Handbook*. Hoboken, NJ: Wiley, 1999. Print.

[2] Koo, J. H. *Polymer Nanocomposites: Processing, Characterization, and Applications*. New York: McGraw-Hill Professional, 2006. Print.

[3] Harper, C. A., and E. M. Petrie. *Plastics Materials Processes: A Concise Encyclopedia.* Hoboken: John Wiley & Sons, 2003. Print.

[4] Mark, H. F. *Encyclopedia of Polymer Science and Technology*. Hoboken, NJ: Wiley-Interscience, 2007. Print.

[5] Piringer, O. G., and Albert Lawrence. Baner. *Plastic Packaging: Interactions with Food and Pharmaceuticals*. Weinheim: Wiley-VCH, 2008. Print.

[6] "Production inches up in most countries." *C&EN*. 7 July 2003. Web. 8 Apr. 2011. <http://pubs.acs.org/cen/coverstory/8127/8127factsfigures.html>.

[7] Sperling, L. H. "Multicomponent Polymeric Materials." *Introduction to Physical Polymer Science*. Hoboken, NJ: Wiley, 2006. Print.

[8] Zhang, M. Q., and M. Z. Rong. "Application of Non-Layered Nanoparticles in Polymer Modification." *Polymer Composites* (2005): 3-22. Web.

[9] Winey, K. I., and R. A. Vaia. "Polymer Nanocomposites." *MRS Bulletin* 32 (2007): 314-22. Print.

[10] Giannelis, E. P. "Polymer Layered Silicate Nanocomposites." *Advanced Materials* 8.1 (1996): 29-35. Print.

[11] Masuda, J., and J. M. Torkelson. "Dispersion and Major Property Enhancements in Polymer/Multiwall Carbon Nanotube Nanocomposites via Solid-State Shear Pulverization Followed by Melt Mixing." *Macromolecules* 41.16 (2008): 5974-977. Print.

[12] Wakabayashi, K., P. J. Brunner, J. Masuda, S. A. Hewlett, and J. M. Torkelson. "Polypropylene-Graphite Nanocomposites Made by Solid-State Shear Pulverization: Effects of Significantly Exfoliated, Unmodified Graphite Content on Physical, Mechanical and Electrical Properties." *Polymer* 51.23 (2010): 5525-531. Print.

[13] Hubert, P. J., K. Kathiresan, and K. Wakabayashi. "Filler Exfoliation and Dispersion in Polypropylene/As-Received Graphite Nanocomposites via Cryogenic Milling." *Submitted To Polymer Engineering Science* (2010). Print.

[14] Pujari, S., T. Ramanathan, K. Kasimatis, J. Masuda, R. Andrews, J. M. Torkelson, L. C. Brinson, and W. R. Burghardt. "Preparation and Characterization of Multiwalled Carbon Nanotube Dispersions in Polypropylene: Melt Mixing Versus Solid-State Shear Pulverization." *Journal of Polymer Science* 47 (2009): 1426-436. Print.

[15] Sinha Ray, S., and M. Okamoto. "New Polylactide/Layered Silicate Nanocomposites, 6." *Macromolecular Materials and Engineering* 288.12 (2003): 936-44. *Wiley Online Library*. Web. 16 Jan. 2011.

[16] LeBaron, P. C., Z. Wang, and T. J. Pinnavaia. "Polymer-layered Silicate Nanocomposites: an Overview." *Applied Clay Science* 15.1-2 (1999): 11-29. *ScienceDirect*. Web. 15 Jan. 2011.

[17] Breuer, O., and U. Sundararaj. "Big Returns from Small Fibers: A Review of Polymer/carbon Nanotube Composites." *Polymer Composites* 25.6 (2004): 630-45. *Wiley Online Library*. Web. 15 Jan. 2011.

[18] Ajayan, P. M., L. S. Schadler, C. Giannaris, and A. Rubio. "Single-Walled Carbon Nanotube-Polymer Composites: Strength and Weakness." *Advanced Materials* 12.10 (2000): 750-53. *Wiley Online Library*. Web. 16 Jan. 2011.

[19] Choudalakis, G., Gotsis, A. D. "Permeability of polymer/clay nanocomposites: A review." *Macromolecular Nanotechnology - Review,* 45, (2009): 967-984.

[20] Nielsen, L. E. "Models for the permeability of filled polymer systems." *Journal of Macromolecular Science,* A1, (1967): 929-942.

[21] Fielding, A. S. “Characterization of Biodegradable Polymer Nanocomposites Fabricated Using Solid-State Processing.” Master of Science Thesis, Bucknell University, 2011.

[22] Shen, J., X. Chen, and W. Huang. "Structure and Electrical Properties of Grafted Polypropylene/graphite Nanocomposites Prepared by Solution Intercalation." *Journal of Applied Polymer Science* 88.7 (2003): 1864-869. *Wiley Online Library*. Web. 11 Feb. 2011.

[23] Park, C., Z. Ounaies, K. A. Watson, R. E. Crooks, J. Smith Jr., S. E. Lowther, J. C. Connell, E. J. Siochi, J. S. Harrison, and T. L. St. Clair. "Dispersion of Single Wall Carbon Nanotubes by in Situ Polymerization under Sonication." *Chemical Physics Letters* 364.3-4 (2002): 303-08. *ScienceDirect*. Web. 23 Jan. 2011.

[24] Hu, G., C. Zhao, S. Zhang, M. Yang, and Z. Wang. "Low Percolation Thresholds of Electrical Conductivity and Rheology in Poly(ethylene Terephthalate) through the Networks of Multi-walled Carbon Nanotubes." *Polymer* 47.1 (2006): 480-88. *ScienceDirect*. Web. 21 Jan. 2011.

[25] Du, F., J. E. Fischer, and K. I. Winey. "Coagulation Method for Preparing Single-walled Carbon Nanotube/poly(methyl Methacrylate) Composites and Their Modulus, Electrical Conductivity, and Thermal Stability." *Journal of Polymer Science Part B: Polymer Physics* 41.24 (2003): 3333-338. *Wiley Online Library*. Web. 22 Jan. 2011.

[26] Safadi, B., R. Andrews, and E. A. Grulke. "Multiwalled Carbon Nanotube Polymer Composites: Synthesis and Characterization of Thin Films." *Journal of Applied Polymer Science* 84.14 (2002): 2660-669. *Wiley Online Library*. Web. 20 Jan. 2011.

[27] Haggenmueller, R., H. H. Gommans, A. G. Rinzler, J. E. Fischer, and K. I. Winey. "Aligned Single-wall Carbon Nanotubes in Composites by Melt Processing Methods." *Chemical Physics Letters* 330.3-4 (2000): 219-25. *ScienceDirect*. Web. 23 Feb. 2011.

[28] Park, S. J., M. S. Cho, S. T. Lim, H. J. Choi, and M. S. Jhon. "Synthesis and Dispersion Characteristics of Multi-Walled Carbon Nanotube Composites with Poly(methyl Methacrylate) Prepared by In-Situ Bulk Polymerization." *Macromolecular Rapid Communications* 24.18 (2003): 1070-073. *Wiley Online Library*. Web. 12 Feb. 2011.

[29] Sung, J. H., H. S. Kim, H. J. Jin, H. J. Choi, and I. J. Chin. "Nanofibrous Membranes Prepared by Multiwalled Carbon Nanotube/Poly(methyl Methacrylate) Composites." *Macromolecules* 37.26 (2004): 9899-902. Print.

[30] McClory, C., T. McNally, G. P. Brennan, and J. Erskine. "Thermosetting Polyurethane Multiwalled Carbon Nanotube Composites." *Journal of Applied Polymer Science* 105.3 (2007): 1003-011. *Wiley Online Library*. Web. 11 Feb. 2011.

[31] Mitchell, C., and R. Krishnamoorti. "Non-isothermal Crystallization of in Situ Polymerized Poly(ε-caprolactone) Functionalized-SWNT Nanocomposites." *Polymer* (2005). *ScienceDirect*. Web. 11 Feb. 2011.

[32] Abdelgoad, M., and P. Potschke. "Rheological Characterization of Melt Processed Polycarbonate-multiwalled Carbon Nanotube Composites." *Journal of Non-Newtonian Fluid Mechanics* 128.1 (2005): 2-6. *ScienceDirect*. Web. 11 Feb. 2011.

[33] Thostenson, E. T., and T. W. Chou. "Aligned Multi-walled Carbon Nanotube-reinforced Composites: Processing and Mechanical Characterization." *Journal of Physics D: Applied Physics* 35.16 (2002): L77-80. *IOP Science*. Web. 15 Jan. 2011.

[34] Kashiwagi, T., E. Grulke, J. Hilding, R. Harris, W. Awad, and J. Douglas. "Thermal Degradation and Flammability Properties of Poly(propylene)/Carbon Nanotube Composites." *Macromolecular Rapid Communications* 2.3 (2002): 761-65. Print.

[35] Kharchenko, S. B., J. F. Douglas, J. Obrzut, E. A. Grulke, and K. B. Migler. "Flow-induced Properties of Nanotube-filled Polymer Materials." *Nature Materials* 3.8 (2004): 564-68. *Nature*. Web. 16 Jan. 2011.

[37] Kim, J. Y., and S. H. Kim. "Influence of Multiwall Carbon Nanotube on Physical Properties of Poly(ethylene 2,6-naphthalate) Nanocomposites." *Journal of Polymer Science Part B: Polymer Physics* 44.7 (2006): 1062-071. *Wiley Online Library*. Web. 30 Mar. 2011.

[37] Furgiuele, N., A. H. Lebovitz, K. Khait, and J. M. Torkelson. "Novel Strategy for Polymer Blend Compatibilization: Solid-State Shear Pulverization." *Macromolecules* 33.2 (2000): 225-28. Print.

[38] Henry, M.. "Solid-state Compatibilization of Immiscible Polymer Blends: Cryogenic Milling and Solid-state Shear Pulverization." Master of Science Thesis, Bucknell University, 2010.

[39] Lyondell Basell. *Petrothene LR7320 High Density Polyethylene*. Technical Information. Print.

[40] DOW. *DOWLEX 2027G Polyethylene Resin*. Technical Information. Print.

[41] Nanocor. *Polymer Grade Montmorillonites*. Technical Information. Print.

[42] Sinha Ray, S., K. Yamada, M. Okamoto, Y. Fujimoto, A. Ogami, and K. Ueda. "New Polylactide/layered Silicate Nanocomposites. 5. Designing of Materials with Desired Properties." *Polymer* 44.21 (2003): 6633-646. *Wiley Online Library*. Web. 25 Mar. 2011.

[43] Okamoto, M. "Biodegradable Polymer/Layered Silicate Nanocomposites: A Review." *Journal of Industrial and Engineering Chemistry* 10 (2004): 1156-181. *Wiley Online Library*. Web. 26 Mar. 2011.

[44] Alexandre, M., and P. Dubois. "Polymer-layered Silicate Nanocomposites: Preparation, Properties and Uses of a New Class of Materials." *Materials Science and Engineering: R: Reports* 28.1-2 (2000): 1-63. *ScienceDirect*. Web. 25 Mar. 2011.

[45] Southern Clay Products. *Cloisite 15A: Typical Physical Properties Bulletin*. Technical Information. Print.

[46] Hwu, J. M., G. J. Jiang, Z. M. Gao, W. Xie, and W. P. Pan. "The Characterization of Organic Modified Clay and Clay-filled PMMA Nanocomposites." *Journal of Applied Polymer Science* 83.8 (2002): 1702-710. Print.

[47] Ray, S. S.; Okamoto, M. "Biodegradable Polylactide and Its Nanocomposites: Opening a New Dimension for Plastics and Composites." *Macromolecular Rapid Communication,* **24**, (2003): 815-840.

[48] "Twin Screw Extruder." *Qingdao Yifeng Plastic Machinery Co.* 29 Dec. 2009. Web. 3 Apr. 2011. <http://www.f9002.cn/plastic/Twin-screw-extruder.html>.

[49] Callister, Jr., W. D., and D. G. Rethwisch. "Mechanical Properties." *Fundamentals of Material Science and Engineering: An Integrated Approach*. 3rd ed. John Wiley & Sons, 2008. 186-241. Print.

[50] Hubert, P. J.. "Solid-State Fabrication and Characterization of Polymer-Graphite Nanocomposites." Master of Science Thesis, Bucknell University, 2009.

[51] Alexander, L. E. *X-ray Diffraction Methods in Polymer Science*. Hoboken, NJ: John Wiley, 1969. Print.

[52] Kakudo, M., and N. Kasai. *X-ray Diffraction by Polymers*. Tokyo: Kodansha, 1972. Print.

[53] Alexandre, M., P. Dubois, T. Sun, J. M. Garces, and R. Jerome. "Polyethylene-layered Silicate Nanocomposites Prepared by the Polymerization-filling Technique: Synthesis and Mechanical Properties." *Polymer* 42.8 (2002): 2123-132. *ISI Web of Knowledge*. Web. 9 Apr. 2011.

[54] Gopakumar, T. G., J. A. Kontopoulou, and J. S. Parent. "Influence of Clay Exfoliation on the Physical Properties of Montmorillonite/polyethylene Composites." *Polymer* 43.20 (2002): 5483-491. *ISI Web of Knowledge*. Web. 10 Apr. 2011.

[55] Hotta, S., and D.R. Paul. "Nanocomposites Formed from Linear Low Density Polyethylene and Organoclays." *Polymer* 45.22 (2004): 7639-654. Web. 9 Apr. 2011.

[56] Wang, K. "Synthesis and Characterization of Maleated Polyethylene/clay Nanocomposites." *Polymer* 42.24 (2001): 9819-826. *ISI Web of Knowledge*. Web. 10 Apr. 2011.

[57] Shah, R., and D. Paul. "Organoclay Degradation in Melt Processed Polyethylene Nanocomposites." *Polymer* 47.11 (2006): 4075-084. *Science Direct*. Web. 10 Apr. 2011.

[58] Liang, G., J. Xu, S. Bao, and W. Xu. "Polyethylene/maleic Anhydride Grafted Polyethylene/organic-montmorillonite Nanocomposites. I. Preparation, Microstructure, and Mechanical Properties." *Journal of Applied Polymer Science* 91.6 (2004): 3974-980. *Science Direct*. Web. 11 Apr. 2011.